



# Kriging-sparse Polynomial Dimensional Decomposition surrogate model with adaptive refinement

Pietro Marco Congedo, Andrea Cortesi, Ghina El Jannoun

## ► To cite this version:

Pietro Marco Congedo, Andrea Cortesi, Ghina El Jannoun. Kriging-sparse Polynomial Dimensional Decomposition surrogate model with adaptive refinement. [Research Report] RR-9098, INRIA Bordeaux, équipe CARDAMOM. 2017. hal-01610195

**HAL Id: hal-01610195**

**<https://inria.hal.science/hal-01610195>**

Submitted on 4 Oct 2017

**HAL** is a multi-disciplinary open access archive for the deposit and dissemination of scientific research documents, whether they are published or not. The documents may come from teaching and research institutions in France or abroad, or from public or private research centers.

L'archive ouverte pluridisciplinaire **HAL**, est destinée au dépôt et à la diffusion de documents scientifiques de niveau recherche, publiés ou non, émanant des établissements d'enseignement et de recherche français ou étrangers, des laboratoires publics ou privés.



# Kriging-sparse Polynomial Dimensional Decomposition surrogate model with adaptive refinement

Andrea F. Cortesi , Pietro M. Congedo

**RESEARCH  
REPORT**

**N° 9098**

August 1 2017

Project-Teams Cardamom





# Kriging-sparse Polynomial Dimensional Decomposition surrogate model with adaptive refinement

Andrea F. Cortesi <sup>\*</sup>, Pietro M. Congedo<sup>†</sup>

Project-Teams Cardamom

Research Report n° 9098 — August 1 2017 — 47 pages

**Abstract:** Uncertainty Quantification and global Sensitivity Analysis problems are made more difficult in the case of applications which involve expensive computer simulations. This because a limited amount of simulations is available to build a sufficiently accurate metamodel of the quantities of interest.

In this work, a numerical technique for the construction of a low-cost and accurate metamodel is proposed, having in mind applications with expensive computer codes. Two main points are introduced. Firstly, a technique which couples Universal Kriging with sparse Polynomial Dimensional Decomposition (PDD) to build a metamodel with improved accuracy. The polynomials selected by the adaptive PDD representation are used as a sparse basis to build an Universal Kriging surrogate model. The second is a strategy, derived from anisotropic mesh adaptation, to adaptively add a fixed number of new training points to an existing Design of Experiments.

The convergence of the proposed algorithm is analyzed and assessed on different test functions with an increasing size of the input space. Finally, the algorithm is used to propagate uncertainties in two high-dimensional real problems related to the atmospheric reentry.

**Key-words:** Surrogate Modeling, Universal Kriging, sparse Polynomial Dimensional Decomposition, Anisotropic Adaptive Meshing, Adaptive Refinement

---

<sup>\*</sup> INRIA Bordeaux Sud-Ouest, 200 Rue de la Vieille Tour, 33405 Talence, France

<sup>†</sup> INRIA Bordeaux Sud-Ouest, 200 Rue de la Vieille Tour, 33405 Talence, France

**RESEARCH CENTRE  
BORDEAUX – SUD-OUEST**

351, Cours de la Libération  
Bâtiment A 29  
33405 Talence Cedex

# Construction d'une fonction substitue base sur un couplage Kriging/"Sparse Polynomial Decomposition" avec raffinement adaptatif

**Résumé :** La quantification des incertitudes et l'analyse de sensibilité sont plus difficiles dans le cas d'applications impliquant des simulations numériques coûteuses. Dans ce travail, une technique numérique pour la construction d'un métamodèle peu coteux et précis est proposée, compte tenu des applications avec des codes numériques coûteux. Deux points principaux sont introduits. Tout d'abord, une technique est proposée pour coupler le Kriging universel au PDD pour construire un métamodèle avec une meilleure précision. La deuxième contribution est une stratégie, dérivée de l'adaptation de maillage, pour ajouter de manière adaptative un nombre fixe de nouveaux points à un plan d'expérience existant.

La convergence de l'algorithme proposé est analysée et évaluée sur différents cas-tests avec une taille croissante de l'espace d'entrée. Enfin, l'algorithme est utilisé pour propager des incertitudes dans deux problèmes réels de haute dimension liés à la rentrée atmosphérique.

**Mots-clés :** Fonction substitue, Universal Kriging, sparse Polynomial Dimensional Decomposition, adaptation de maillage.

## Contents

<b>1</b>	<b>Introduction</b>	<b>3</b>
<b>2</b>	<b>Starting point in metamodeling</b>	<b>7</b>
2.1	Regression-based adaptive sparse-PDD . . . . .	8
2.1.1	Classical PDD representation . . . . .	8
2.1.2	Dimension reduction for the model representation . . . . .	9
2.2	Universal Kriging surrogate . . . . .	11
<b>3</b>	<b>PDD-UK surrogate model and adaptive sampling</b>	<b>12</b>
3.1	Choice of the basis and PDD-UK based surrogate construction . . . . .	13
3.2	Adaptive sampling through anisotropic mesh adaptation . . . . .	15
3.2.1	Basic Algorithm . . . . .	15
3.2.2	Error criterion . . . . .	16
3.2.3	Refinement by adding a fixed number of points . . . . .	17
3.2.4	Extrapolation technique for higher-dimensional input spaces . . . . .	20
3.3	Parameters of interest . . . . .	20
<b>4</b>	<b>Numerical experiments</b>	<b>21</b>
4.1	Results without mesh adaptation . . . . .	22
4.1.1	<b>TEST 1:</b> 2D function . . . . .	22
4.1.2	<b>TEST 2:</b> Ishigami function . . . . .	22
4.1.3	<b>TEST 3:</b> 8D Sobol function . . . . .	25
4.1.4	<b>TEST 4:</b> 100D Sobol function . . . . .	26
4.2	Assessment of the adaptive strategy . . . . .	28
4.2.1	Comparison between brute and fast approach . . . . .	29
4.2.2	Convergence . . . . .	29
4.3	Engineering Applications . . . . .	30
4.3.1	EXPERT reentry . . . . .	30
4.3.2	TACOT ablation test case . . . . .	32
<b>5</b>	<b>Conclusions</b>	<b>34</b>
<b>A</b>	<b>Metamodel assessment</b>	<b>35</b>
<b>B</b>	<b>Sensitivity Indices</b>	<b>36</b>

## 1 Introduction

A wide range of applications in the field of applied mathematics and engineering rely on the numerical solution of complex mathematical models. Today, with the important advancements in numerical modeling and the increasing computer powers, highly accurate simulations of complex physical phenomena can be obtained, often at a price of a prohibitive computational cost. Moreover, the computational burden can dramatically rise when several solution evaluations with different configurations or different parameters are needed, for example in (stochastic) design optimization, Bayesian inference, Uncertainty Quantification (UQ) or global Sensitivity Analysis (gSA). A common practice in these fields is to perform a limited amount of exact evaluations of the solution and then use

the obtained values to build a surrogate model, able to emulate the output of the complex model in other points than the observed ones.

Ideally, a surrogate model should be able to give a good representation of the quantity of interest while reducing as much as possible the discrepancy error between the approximate and the exact function. Nevertheless, in order to build up an efficient model, the developed numerical method should reduce to the minimum the number of direct true model evaluations which are very expensive computationally.

The problem of building a cheap metamodel able to give an accurate approximation of the real function is not trivial. Several techniques have been explored in the literature. Generic and more application-oriented techniques were proposed. An ongoing effort is still performed to improve their accuracy and efficiency, especially in the case of high-dimensional real-life problems, where many classical metamodeling methods still require a drastic number of model evaluations. Some examples of surrogate models include polynomial response surfaces [1], Polynomial Chaos expansion [2, 3], Polynomial Dimensional Decomposition [4], Radial Basis Functions [5] and Kriging [6]. Kriging is also known in literature as Gaussian Process regression [7]. It is based on the main idea of considering the function of interest as a realization of a stationary Gaussian stochastic process. The method is now popular as a metamodeling technique in different research fields of applied mathematics, such as global optimization and uncertainty quantification [8] [9, 10] [11] [12]. As pointed out in [13], often in practical applications, Kriging is mostly used in its basic configuration known as Ordinary Kriging, because of the lack of *a priori* knowledge about the main trends of the function of interest. In this way the efficiency and the accuracy of the method are reduced with respect to its prospective. for the Universal Kriging.

In a recent work, Kersaudy et al. [13] proposed to combine Universal Kriging with a different metamodeling technique, known as LARS Polynomial Chaos, which is able to find a good basis function for the regression term, leading to a more accurate metamodel with the same size of the design of experiments. In another previous work, the blind-Kriging method [14] was developed. It shares some similarities with the work in [13], but employs a Bayesian selection algorithm for the selection of basis functions.

The first main contribution of this paper is to take the cue from [13] and use the functions chosen by a first metamodeling technique for the regression term of Universal Kriging. The difference is that the sparse Polynomial Dimensional Decomposition, in the adaptive implementation developed by Tang et al. [15], is used as first surrogate. Polynomial Dimensional Decomposition (PDD) [4] is a technique for building a hierarchical decomposition of a multivariate function. It directly relies on the well-known ANOVA functional decomposition [16, 17] and they both share a close structure. In this way, the PDD is able to give the priority to exploit low-order parameter interactions, following the principle where low-order ANOVA component functions are dominant for most engineering cases. For this reason, PDD is preferred over Polynomial Chaos (PC) expansion in this work. In fact, as pointed out in [18], if a (stochastic) function is highly nonlinear, but contains rapidly diminishing interaction effects of multiple variables, the PDD approximation is expected to be more effective than the PC approximation, as the lower-variate interaction terms of the PDD approximation can be just as nonlinear by selecting appropriate values of maxi-

mum polynomial degree in the PDD. However, many more terms and expansion coefficients must be included in the PCE approximation to capture such a high nonlinearity. In [15], the authors proposed an adaptive sparse implementation of the PDD that showed to produce good results for sensibility analysis, thus being able to efficiently capture the main trends of the function. The purpose of the coupling between Kriging and sparse-PDD is then to start from the surrogate produced by the sparse-PDD, able to follow the main trends of the function, and exploit the Kriging to add a correction that improves the quality of the metamodel and leads to an interpolating metamodel, at least when not considering the nugget effect in the covariance of the Gaussian process. Of course the training cost of the coupled technique will be higher with respect to each single normal method, but for expensive real-world applications it would be lower than the cost of a single evaluation of the complex model.

Another aspect that has a significant impact on the final quality of the metamodel is the choice of the Design of Experiments (DoE) (or Experimental Design), i.e. the set of sampling points (or training points) on which the real model is evaluated, and that are used to train the surrogate. A method for efficiently adding training points to the initial DoE can be useful to improve the accuracy without discarding the previous model evaluations and the information acquired on the function of interest and metamodeling error. In literature, a big effort has been done on how to determine the best position of the initial experimental design and on how to refine it. Often, for the construction of surrogate models, training points are chosen according to space-filling criteria. A straightforward way to generate an experimental design with this characteristic is Latin Hypercube Sampling (LHS) [19]. This kind of DoE is widely used with good results. For example, in the well known DACE algorithm [20], one of the proposed methods to create the Experimental Design is Latin Hypercubes sampling. Improvements have been performed in [21] by coupling the generation of a LHS design with optimality criteria for Kriging training points. Techniques have also been developed to increase the number of points of an already existing design while keeping its good space-filling properties, for example the nested Latin Hypercube sampling introduced in [22]. This kind of methods however does not account for any information regarding the function of interest to enrich the DoE.

For Kriging response surfaces, different techniques have been investigated to create and enrich set of training points in such a way that the metamodeling error is reduced. For example, in [23], the Maximum Mean Squared Error (MMSE), Integrated Mean Squared Error (IMSE) or an entropy criteria are used to create and sequentially increment the design of experiment in such a way that is possible to optimize the metamodeling error, which is considered to be the variance of the Gaussian process. However, it is important to remind that the Kriging variance is a model-based estimate of the metamodeling error, and it is more an indicator of the good distribution of the training points in the domain. In some cases it is possible that it is not a good estimate of the true metamodeling error. Furthermore, it does not depend directly on the evaluations of the function of interest.

Sometimes, since the function of interest could present a behavior which is just locally more difficult to represent by means of a surrogate model, it could be useful to rely on some adaptive technique able to add a certain amount of points to the initial set of training points in the most problematic regions. In fact, for



example using a space filling refinement, the algorithm would add points in all the domain, including those areas where the function is more regular and does not need further evaluations to be well represented, thus leading to a waste of computational resources. Whereas, an adaptive strategy for the selection of new training points could improve the final quality of the metamodel containing the number of model evaluations.

Finding an adequate way to use the information about the already evaluated training points to globally and adaptively improve the metamodel accuracy is not straightforward. Some examples of adaptive designs can be found in the literature. They are often focused on a special purpose or linked to specific techniques. For example, in the work of Witteveen about Simplex Stochastic Collocation (SSC) [24, 25, 26, 27], an adaptive refinement strategy is proposed and developed to add simplex elements in the probability space. This allows to refine the discretization of the stochastic space according to an error indicator based on the hierarchical residual of the stochastic collocation (and also other indicators) in order to deal with complex functions which can also show discontinuous behaviors in the response surface.

The second major contribution of this paper is to introduce an adaptation method which adds new points to the Experimental Design in the view of improving the efficiency and accuracy of the computations. It builds upon the idea of building an  $n$ -dimensional Delaunay triangulation on the training points and then apply a mesh adaptation technique.

Several mesh adaptation techniques were proposed in the literature in the context of metamodeling. Among these methods one can find the Mesh Adaptive Direct Search (MADS) algorithm [28]. Although these methods provided good approximations for small dimensional problems, their convergence rate can be very slow for higher dimensions as they rely on the function values without fully exploiting the inherent smoothness of the objective function.

Metamodeling node insertion techniques based on either global or local search algorithms can be found in the literature. Gutmann [29] proposed a node selection method that relies on the minimization of a "bumpiness" measure whereas Regis and Shoemaker [30, 31] proposed an optimization approach that starts from a feasible random set of points then takes small step sizes and search for the points that best represent the metamodel function values. Jakobsson et al. [32] proposed an adaptation method that controls the total uncertainty. On the other hand, local search algorithms move toward a locally optimized solution. Although these optimization techniques were based on a robust theoretical basis and successfully applied to expensive functions, they induce a relatively important computational cost.

In [25], the authors derived a rigorous stopping criterion for  $h$ -refinement. The proposed method relies on a robust mathematical foundation. However, two efficiency bottlenecks of these methods can be detected. First, they do not consider any control on the mesh complexity as a function of the available computational resources. Second, they do not take advantage of the directional aspect of the functional gradient and hence apply the same refinement in all the directions.

The adaptation method adopted in this work exploits a mesh adaptation technique [33, 34], developed in the context of Computational-Fluid-Dynamics (CFD) applications, to derive an algorithm which adds new training points along the edges of the grid according to the optimization of an error criterion. Nodes

are added to the grid, where the training function presents sharp gradients in order to better capture the variation of the function all over the domain. As a consequence, the proposed algorithm starts by measuring the error along the edges of the mesh as a function of the gradient variation. Then in order to quadratically minimize the total error it optimally inserts new nodes along these edges under the constraint of a fixed number of nodes. Unlike derivative-free optimization methods [28, 35], the newly developed algorithm uses the information about the function smoothness in order to converge faster to the optimal solution.

It is important to mention that a major feature of the proposed mesh adaptation technique is that it is not constrained to a specific metamodeling technique or experimental design.

Compared to the above cited adaptation techniques, the proposed approach is fast and very simple to apply as it only requires the values of the function on the grid points and a fixed number of additional nodes imposed by the user. The latter criterion is an asset for efficiency and accuracy. Given the computational power at hand, the user can fix a certain maximal mesh complexity and the algorithm will adapt to provide the optimal accuracy with that number of nodes. This is an advantage with respect to other adaptation methods [25, 18] that rely on a desired accuracy which most of the time cannot be reached due to the lack of computational power or memory capacity. In that case the other approaches try to lower the imposed accuracy then restart the computations.

Finally, the directional feature of the refinement as well as its multi-component nature are key assets of the developed method that make it outperform classical uniform, structured and isotropic mesh refinement techniques found in the literature [25, 18].

The paper is organized as follows. In Section 2, a synthetic description of adaptive Sparse PDD (2.1) and Universal Kriging (2.2) is provided. Note that in A some techniques are proposed for the metamodel assessment. Then, Section 3 illustrates the approach proposed in this paper for the construction of a robust surrogate model. Section 3.1 describes the coupling between the PDD basis functions with the regression term in Universal Kriging. Afterwards, Section 3.2 describes the proposed adaptive sampling, which is further developed in Section 3.2.3 and ???. Some results of convergence on different test functions are presented in Section 4.1, while Section 4.2 is focused on the adaptive sampling technique. Finally, in Section 4.3, the algorithm is applied to two engineering problems in aerospace. Section 5 draws some conclusions and considerations on future developments.

## 2 Starting point in metamodeling

Let us suppose to have a  $N$  dimensional input random variable  $\mathbf{X} = \{X_1, \dots, X_N\}$  with a joint probability density function (PDF)  $p_{\mathbf{X}}(\mathbf{x})$ . The assumption of independence of the components of this random vector implies that its PDF can be written as

$$p_{\mathbf{X}}(\mathbf{x}) = \prod_{i=1}^N p_{X_i}(x_i) \quad (1)$$

where  $p_{X_i}(x_i)$  is the marginal PDF of  $X_i$ .

Let us suppose that the response of a given system can be represented by a  $N$ -dimensional function of interest  $y = f(\mathbf{x})$ . Different engineering problems, such as optimization or uncertainty quantification, may require several evaluations of the function of interest at different values of  $\mathbf{x}$ . However, this may be very expensive to be evaluated, for example in complex computational models based on partial differential equations. Therefore, in this cases, one can resort to using a cheap surrogate model  $\hat{f}(\mathbf{x})$  to predict the value of the quantity of interest.

## 2.1 Regression-based adaptive sparse-PDD

Here, the sparse-Polynomial Dimensional Decomposition (sPDD) technique implementation used in this work is recalled. This adaptive strategy to build a PDD metamodel with the sparse approach has been proposed by Tang et al. in a recent work [15]. In the original paper, the technique addresses primarily to problems of global sensitivity analysis and uncertainty quantification, but it can be employed also as a surrogate model representation of the function of interest for other applications.

### 2.1.1 Classical PDD representation

Let us briefly recall the ANOVA representation of a multivariate function. More details can be found, for example, in [16, 17]. In general, the multivariate function of interest can be represented by the following expansion:

$$y = f(\mathbf{x}) = f_0 + \sum_{s=1}^N \sum_{i_1 < \dots < i_s} f_{i_1 \dots i_s}(x_{i_1}, \dots, x_{i_s}) \quad (2)$$

which can be rewritten in compact form exploiting a multi index notation:

$$y = f_{s_0} + \sum_{j=1}^{\mathcal{M}} f_{s_j}(\mathbf{x}_{s_j}) \quad \text{with} \quad \mathcal{M} = 2^N - 1 \quad (3)$$

This representation is called ANOVA (Analysis of Variance) decomposition if, for any  $j \in 1, \dots, \mathcal{M}$ , the following orthogonality condition is respected

$$\int_{\mathbb{R}} f_{s_j}(\mathbf{x}_{s_j}) p_{X_i}(x_i) dx_i = 0 \quad \text{for} \quad x_i \in \{\mathbf{x}_{s_j}\} \quad (4)$$

Some interesting properties of the ANOVA decomposition are shown in [15].

Until this point, the component functions  $f_{s_j}$  of the ANOVA decomposition of the function of interest are not determined yet. In literature, two techniques are mainly used at this purpose: Polynomial Chaos expansion (PC) and Polynomial Dimensional Decomposition (PDD). As shown in [18, 15], the PDD could be preferred for its closer structure with respect to ANOVA.

Let us consider then an orthogonal set of polynomials in the Hilbert space  $\mathcal{L}_2$ , denoted by  $\{\psi_j(x_i); j = 0, 1, \dots\}$ , such that

$$\int_{\mathbb{R}} \psi_j(x_i) \psi_k(x_i) p_{X_i}(x_i) dx_i = \gamma_{j, X_i} \delta_{ij} \quad (5)$$

where  $j$  and  $k$  are the order of the polynomials for the variable  $x_i$  and with the normalization constant  $\gamma_{j,X_i}$  determined as

$$\gamma_{j,X_i} = \int_{\mathbb{R}} \psi_j^2(x_i) p_{X_i}(x_i) dx_i. \quad (6)$$

As well-known in literature (see [4] for example), an optimal choice is to have a basis corresponding to families of polynomials which are orthogonal to some probability distributions.

Let us consider now a  $T$ -dimensional term of the ANOVA decomposition, with  $1 \leq T \leq N$

$$f_{i_1, i_2, \dots, i_T}(x_{i_1}, x_{i_2}, \dots, x_{i_T}) \quad (7)$$

The component function can be expanded as done in [4]:

$$f_{i_1, i_2, \dots, i_T}(x_{i_1}, x_{i_2}, \dots, x_{i_T}) = \sum_{j_T=1}^{\infty} \dots \sum_{j_1=1}^{\infty} C_{i_1, i_2, \dots, i_T}^{j_1, j_2, \dots, j_T} \prod_{k=1}^T \psi_{j_k}(x_{i_k}) \quad (8)$$

In practice the expansion must be truncated, leaving  $m$  terms for each dimension. Thus, the polynomial dimensional decomposition of the function of interest can be written in the following final expression

$$\begin{aligned} f(\mathbf{x}) \simeq \hat{f}_m(\mathbf{x}) = & f_0 + \sum_{i=1}^N \sum_{j=1}^m C_i^j \psi_j(x_i) + \sum_{i_1 < i_2}^N \sum_{j_2=1}^m \sum_{j_1=1}^m C_{i_1, i_2}^{j_1, j_2} \psi_{j_1}(x_{i_1}) \psi_{j_2}(x_{i_2}) + \\ & + \sum_{i_1 < i_2 < i_3}^N \sum_{j_3=1}^m \sum_{j_2=1}^m \sum_{j_1=1}^m C_{i_1, i_2, i_3}^{j_1, j_2, j_3} \psi_{j_1}(x_{i_1}) \psi_{j_2}(x_{i_2}) \psi_{j_3}(x_{i_3}) + \\ & + \dots + \sum_{i_1 < \dots < i_N}^N \sum_{j_N=1}^m \dots \sum_{j_1=1}^m C_{i_1, i_2, \dots, i_N}^{j_1, j_2, \dots, j_N} \prod_{k=1}^N \psi_{j_k}(x_{i_k}) \end{aligned} \quad (9)$$

Hence the total size  $P$  of the  $m$ -th order PDD expansion of an  $N$ -dimensional function is  $P = (1 + m)^N$ . As in [15], a regression approach is preferred to a projection approach for the computation of the coefficients of the expansion  $C_{\dots}$ . This first approach is supposed to be more flexible for problems with a moderate number of variables, but the corresponding surrogate model does not interpolate exactly the training points.

### 2.1.2 Dimension reduction for the model representation

For practical problems, in particular the ones with a moderate to large number of stochastic variables, the size of the PDD expansion becomes very large. For this reason, in [15] an adaptive dimension reduction of the representation has been proposed. This adaptive technique belongs to the family of *stepwise regression*.

Since the lower order interaction terms often have the greater impact on the output, the full ANOVA expansion can be truncated at a maximum dimension of component functions  $\nu < N$ , called the truncation dimension

$$f(\mathbf{x}) = f_0 + \sum_{T=1}^{\nu} \sum_{i_1 < \dots < i_T}^N f_{i_1, i_2, \dots, i_T}(x_{i_1}, x_{i_2}, \dots, x_{i_T}) \quad (10)$$

However, especially for problems with a high dimension of the stochastic space  $N$ , ANOVA decomposition can be still very expensive. This problem can be addressed by using the adaptive ANOVA decomposition

$$f(\mathbf{x}) = f_0 + \sum_{T=1}^{\nu} \sum_{i_1 < \dots < i_T}^{D_T} f_{i_1, i_2, \dots, i_T}(x_{i_1}, x_{i_2}, \dots, x_{i_T}) \quad (11)$$

where  $D_T < N$  is the active dimension of the component function of  $T$ -th order. In this work we will consider  $D_1 = N$  and the active dimension for higher order terms will be determined with the criterion proposed afterwards.

Even with an adapted ANOVA expansion, the computational cost required to compute the classical PDD expansion for each component function is still very high. However, in many real-world problems the contribution of some polynomial terms is negligible with respect to the accuracy of the metamodel or their impact on the global variance. This fact can be exploited to build a sparse PDD representation without compromising the accuracy of the metamodel.

The global adaptive sparse algorithm can be described combining adaptive ANOVA and sparse PDD:

1. Construct a full set of PDD representation (given  $m$ ) for all the first order ANOVA component functions

$$f(\mathbf{x}) \simeq f_0 + \sum_{i=1}^N f_i(x_i) = f_0 + \sum_{i=1}^N \sum_{j=1}^m C_i^j \psi_j(x_i). \quad (12)$$

Compute then the total first order variance (see [15])

$$\text{Var}(f(\mathbf{x})) = \sum_{i=1}^N \sum_{j=1}^m (C_i^j)^2 \gamma_i^j \quad (13)$$

and first order global sensitivity indices

$$\mathcal{S}_i = \frac{\sum_{j=1}^m (C_i^j)^2 \gamma_i^j}{\text{Var}(f(\mathbf{x}))} \quad (14)$$

Assuming the sensitivity indices to be monotonically decreasing ordered with respect to  $i$ , it is possible to choose the active dimension  $D_2$  for second order ANOVA functions such as  $\sum_{i=1}^{D_2} \mathcal{S}_i \geq p$ .

2. Reduce the size of the first order PDD expansion expressed in equation 12, eliminating the less important terms in variance contribution. The obtained first-order reduced basis is denoted by  $\{\psi_{\alpha^1}\}$ .
3. Enrich the model by adding significant higher order terms at the concise first-order basis, obtaining the final basis  $\{\psi_{\alpha^F}\}$ .

In [15], two different algorithms were proposed to choose the most relevant terms to be added to the sparse basis. In the first based on the variance (see algorithm 1), the terms are chosen according to their contribution to the total variance associated to the output function of interest. This algorithm proved to be very effective for the computation of the sensitivity indices. The second algorithm is based on the metamodeling error (see algorithm 2) and instead selects the most relevant terms according to their contribution to the global metamodeling error computed with a leave-one-out cross-validation.

**Algorithm 1** Variance-based adaptive PDD by stepwise regression

---

```

1: Initialization of PDD basis  $\{\psi^w\} = \{\psi_{\alpha^1}\}$ 
2: for  $\psi_{\alpha_i} \in \{\psi_{\alpha^{2+}}\}$  do
3:   add  $\psi_{\alpha_i}$  into  $\{\psi^w\}$ , namely  $\{\psi^w\} = \{\psi^w, \psi_{\alpha_i}\}$ 
4:   solve the regression system to determine the PDD expansion coefficients
5:   compute the total variance  $\text{Var}(f^w(\mathbf{X}))$ 
6:   for  $\psi_{\alpha_j} \in \{\psi^w\}$  do
7:     if  $(C_{\alpha_j})^2 \gamma_{\alpha_j} / \text{Var}(f^w(\mathbf{X})) < \theta$  then
8:       eliminate this polynomial:  $\{\psi^w\} = \{\psi^w\} \setminus \psi_{\alpha_j}$ 
9:     end if
10:  end for
11: end for
12: solve the final regression system based on the constructed basis  $\{\psi^F\}$ 

```

---

**Algorithm 2** Error-based adaptive PDD by stepwise regression

---

```

1: Initialization of PDD basis  $\{\psi^w\} = \{\psi_{\alpha^1}\}$ 
2: for  $\psi_{\alpha_i} \in \{\psi_{\alpha^{2+}}\}$  do
3:   add  $\psi_{\alpha_i}$  into  $\{\psi^w\}$ , namely  $\{\psi^w\} = \{\psi^w, \psi_{\alpha_i}\}$ 
4:   solve the regression system to determine the PDD expansion coefficients
5:   evaluate the metamodel accuracy  $Q_i^2$ 
6:   if  $Q_i^2 \geq Q_{tgt}^2$  then
7:     exit
8:   end if
9:   for  $\psi_{\alpha_j} \in \{\psi^w\}$  do
10:    solve the regression system with the polynomial basis  $\{\psi^w\} \setminus \psi_{\alpha_j}$ 
11:    evaluate the metamodel accuracy  $Q_{i \setminus \alpha_j}^2$ 
12:    if  $Q_i^2 - Q_{i \setminus \alpha_j}^2 < \epsilon_{Q^2}$  then
13:      eliminate this polynomial:  $\{\psi^w\} = \{\psi^w\} \setminus \psi_{\alpha_j}$ 
14:    end if
15:  end for
16: end for
17: solve the final regression system based on the constructed basis  $\{\psi^F\}$ 

```

---

## 2.2 Universal Kriging surrogate

Kriging interpolation [36, 23, 6, 20] is a well-known technique for building a surrogate model. Its main idea is to consider the function of interest  $f(\mathbf{x})$  as a realization of a stationary Gaussian stochastic process  $F(\mathbf{x})$ . In Universal Kriging (UK), the stochastic process can be written in the form of the sum of a deterministic regression model and a stochastic departure term

$$F(\mathbf{x}) = \sum_{j=1}^n \beta_j y_j(\mathbf{x}) + Z(\mathbf{x}) \quad (15)$$

where  $y_j(\mathbf{x})$  are linearly independent known regression functions,  $\beta_j$  are unknown weights, and  $Z(\mathbf{x})$  is a Gaussian process with zero mean and covariance  $k(\mathbf{u}, \mathbf{v})$ . The departure term is assumed to be correlated as a function of the distance between different points, using a prescribed correlation model such as

exponential, Gaussian or Matérn correlation functions [37]. The parameters  $\sigma$  and  $\mathbf{l} = \{l_j\}_{j=1}^N$ , representing respectively the amplitude of the correlation and the correlation lengths, are called *hyperparameters* and enter as known parameters in the construction of the Kriging response surface. For this reason they need to be estimated in a previous step, for example by using the maximum likelihood estimation.

Then the final aim is to build an interpolation of the function of interest in the form

$$\hat{f}(\mathbf{x}) = \sum_{i=1}^{N_s} f(\mathbf{x}_i) \lambda_i(\mathbf{x}) \quad (16)$$

where  $\mathbf{f}_{obs} = (f(\mathbf{x}_1), \dots, f(\mathbf{x}_{N_s}))^T$  are the observations of the function at the  $N_s$  training points (the design of experiment) and  $\lambda_i(\mathbf{x})$  are unknown weights. The best linear unbiased predictor can be obtained by minimizing the mean square error between the model and the predictor  $MSE = E[(F(\mathbf{x}) - \hat{f}(\mathbf{x}))^2]$  under the constraint of unbiasedness  $E[F(\mathbf{x}) - \hat{f}(\mathbf{x})] = 0$ . In this way it is possible to obtain the predictive mean of the stochastic process, that can be used as a metamodel for the original function

$$f(\mathbf{x}) \simeq \hat{f}(\mathbf{x}) = \mu_k(\mathbf{x}) = \mathbf{y}^T(\mathbf{x})\boldsymbol{\beta} + \mathbf{c}(\mathbf{x})^T C^{-1}(\mathbf{f}_{obs} - Y\boldsymbol{\beta}) \quad (17)$$

with  $\boldsymbol{\beta} = (Y^T C^{-1} Y)^{-1} Y^T C^{-1} \mathbf{f}_{obs}$

where  $\mathbf{y}(\mathbf{x}) = (y_1(\mathbf{x}), \dots, y_n(\mathbf{x}))^T$  is the vector of basis functions,  $Y$  is a matrix whose elements are the evaluation of the  $j$ -th basis function at the  $i$ -th training point  $Y_{ij} = y_j(\mathbf{x}_i)$ ,  $\mathbf{c}(\mathbf{x})$  is the vector of correlations between the point  $\mathbf{x}$  and each training point and  $C$  is the matrix of correlations among training points.

It is possible to compute also the predictive variance, which can be used as a local model-based error estimate

$$\sigma^2(\mathbf{x}) = k(\mathbf{x}, \mathbf{x}) + \mathbf{a}(\mathbf{x})^T (Y^T C^{-1} Y)^{-1} \mathbf{a}(\mathbf{x}) - \mathbf{c}(\mathbf{x})^T C^{-1} \mathbf{c}(\mathbf{x}) \quad (18)$$

with  $\mathbf{a}(\mathbf{x}) = Y^T C^{-1} \mathbf{c}(\mathbf{x}) - \mathbf{y}(\mathbf{x})$

In real-world applications, often the Universal Kriging is not used, because it can be difficult to determine relevant basis functions for the regression term in Equation 15 without the proper *a priori* knowledge about the evolution of the quantity of interest. Hence, one is limited to use the simpler technique called *Ordinary Kriging*, in which the regression functions are chosen as  $y_1(\mathbf{x}) = 1$  and  $y_j(\mathbf{x}) = 0$  for  $j \neq 1$ , which means that only a constant regression term is kept and then only  $\beta_1$  needs to be determined. This simplifies the method but can limit the accuracy of the metamodeling technique, thus requiring a higher number of training points in order to obtain a representation of the output function with a certain level of accuracy.

### 3 PDD-UK surrogate model and adaptive sampling

This section illustrates the global algorithm proposed in this paper, named PDD-UK, for the construction of an accurate surrogate model, while having in mind applications where the function of interest is expensive to evaluate. The main points of this procedure are summarized in Algorithm 3.

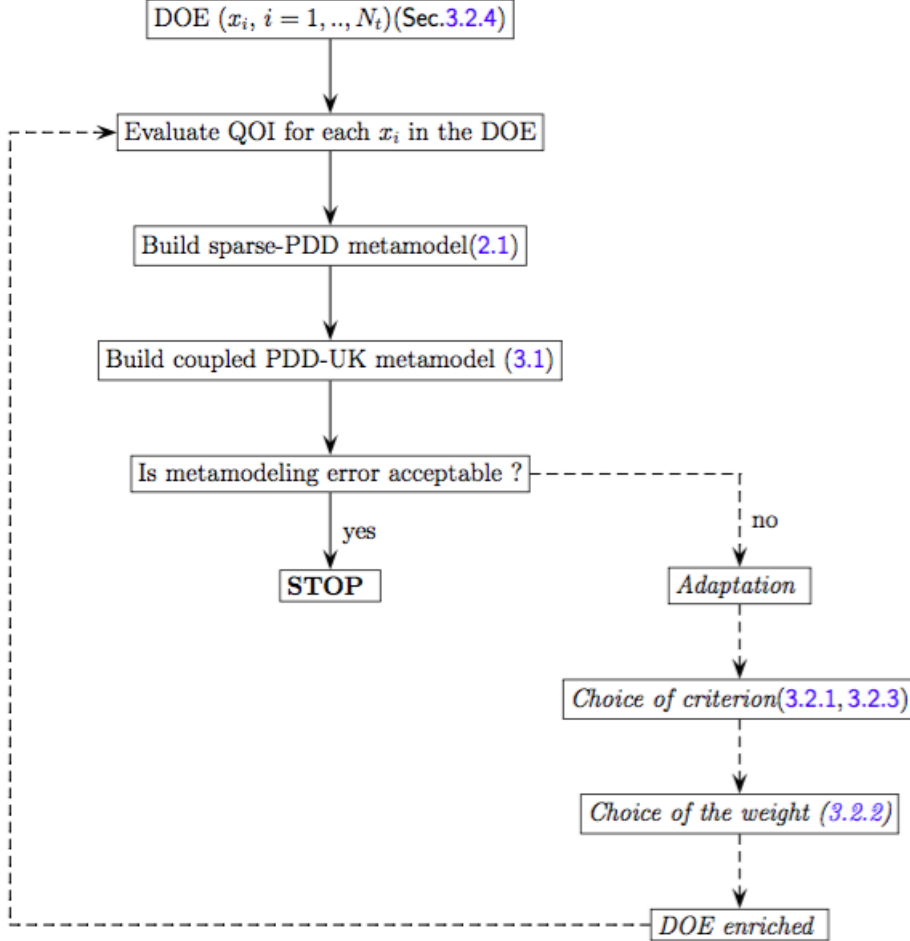


Figure 1: Global metamodeling procedure

First, a coupled PDD-Universal Kriging surrogate is built (see Section 3.1). The goal is to reduce the number of training points required to achieve a desired accuracy. Secondly, the estimated metamodeling error is compared to a given criterion. If not respected, a refinement procedure is applied (see Sections 3.2 and 3.2.3), and Design of Experiments is further enriched with new samples. It consists in treating the training points as nodes of a simplex grid and applying an adaptation method derived from anisotropic adaptive meshing domain.

### 3.1 Choice of the basis and PDD-UK based surrogate construction

As pointed out by Kersaudy et al. in [13], often the lack of *a priori* knowledge on the function of interest forces to use the Kriging technique in the basic configuration known as Ordinary Kriging (see Section 2.2). They proposed to use a sparse polynomial chaos (PC) expansion computed with LARS algorithm



---

**Algorithm 3** Global metamodeling procedure
 

---

```

1: if extrapolation (3.2.4) then
2:   Create an initial set of training points (DoE) in the input space
3: else
4:   Create an initial DoE in the input space + corners
5: end if
6: while unacceptable metamodeling error do
7:   Evaluate the function of interest in the training points
8:   Build the sparse-PDD metamodel to get the basis functions (2.1)
9:   Build the coupled PDD-UK metamodel (3.1)
10:  Estimate the metamodeling error
11:  if adaptation then
12:    Chose whether the number of added points should be fixed (3.2.3) or
    not (3.2.1)
13:    Tune the weight between Kriging and gradient-based error (3.2.2)
14:    Adaptively refine the DoE (with extrapolation if necessary)
15:  end if
16: end while

```

---

to obtain a set of regression functions to build an Universal Kriging surrogate model.

In this paper, the basis is chosen by applying the adaptive sparse PDD algorithm (Sec. 2.1). This is a very sparse representation of the function of interest that is able to achieve a good metamodeling accuracy and to discard the stochastic variables whose influence on the output value is negligible. Then, the basis is used as a regression function for the Universal Kriging surrogate model. The use of the most influential polynomials as basis for the Universal Kriging should improve the quality of the final surrogate by adding the most relevant information about the trends of the quantity of interest to the regression term.

The algorithm used here to couple Universal Kriging with the sparse-PDD basis functions is the following:

1. Build a design of experiments (set of training points)
2. Perform an adaptive sparse PDD and obtain a set of relevant basis function  $\{\psi_{\alpha^F}\}$ , with the following PDD representation of the function of interest:

$$\hat{f}(\mathbf{x}) = f_0 + \sum_{\alpha \in \alpha^F} C_{\alpha} \psi_{\alpha} \quad \text{with} \quad C_{\alpha} \psi_{\alpha} = C_{i_{\alpha}}^{j_{\alpha}} \psi_{j_{\alpha}}(x_{i_{\alpha}}) \quad (19)$$

where  $i_{\alpha}$  and  $j_{\alpha}$  are respectively multi-indices. Also  $\psi_0 = 1$  must be kept in the set of basis function for the Universal kriging.

3. Train the Kriging surrogate, within a Universal Kriging approach, using the basis functions of the sparse PDD expansion as regression functions

$$F(\mathbf{x}) = \sum_{j \in \alpha^F} \beta_j \psi_j + Z(\mathbf{x}) \quad (20)$$

It must be noticed that the original coupling algorithm of Kersaudy and coworkers is more complex. In fact, it builds a UK metamodel at each step of the cycle used to enrich the sparse PC basis and computes cross validation error for each metamodel, then choses the best metamodel according to the error. Even if this approach could lead to further improvements of the quality of the metamodel, it seems quite complex and computationally expensive, especially for high dimensional functions where a lot of polynomial terms are required in the sparse PDD representation. However, this difference in the implementation does not change the main idea of the coupling process, and this feature could always be added later.

In cases where just a subset of the input variables contributes for the most to the variation of the output, it could be possible to reduce the size of the input to facilitate the training of the surrogate model, thus improving its quality. The simple strategy that can be exploited in the framework proposed in this work consists in building the final UK considering as input variables just the ones whose total sensitivity index, computed with sparse-PDD, is non-null. In this way all the inputs which show an irrelevant contribution to the output are neglected, simplifying the training problem and the fitting of the hyperparameters. Other techniques for the input size reduction and their coupling with Kriging surrogate models have been developed in literature. Two examples are the Active Subspaces method [38] and anchored-ANOVA [39], but the in-deep analysis and comparison are not object of study in this paper. The dimension reduction strategy test will be just proposed for the 100-dimension Sobol function 4.1.4 and the TACOT ablation engineering case 4.3.2.

### 3.2 Adaptive sampling through anisotropic mesh adaptation

One critical aspect in the accuracy of metamodels is the construction of a good set of training points. Often in literature, points are chosen according to space-filling criteria, such as Latin Hypercubes designs. However, in some applications, the total number of available evaluations of the accurate model can be limited by its elevated computational cost, and a first surrogate model built on this small design of experiments could show a lower accuracy than desired. In this section, we present a method for efficiently adding training points to the initial DoE, without discarding the previous model evaluations and exploiting the information acquired on the function of interest and metamodeling error.

#### 3.2.1 Basic Algorithm

The adaptation method proposed in this work is based on the building of a mesh of simplex elements in the stochastic space of the input parameters, considering the training points as nodes of the elements, and on the exploitation of an extended mesh adaptation technique, derived from CFD applications.

In particular, new training points are added along the edges of the grid according to the optimization of an error criterion. Note that this helps avoiding an excessive clustering of new points around the area which defines the optimum of the adaptation criterion, even if adding nodes just on the edges leads to a non optimality of the methodology. The drawback of this technique is the fact that it relies on the notion of edges of a mesh, and, as known, the construction

of an  $n$ -dimensional Delaunay triangulation for higher dimensional spaces can become very costly.

A first simple implementation of the algorithm is directly derived from the work of Coupez et al. [33, 34] on anisotropic adaptive meshing. With the original algorithm from Coupez, the total number of mesh nodes is fixed by the user and does not change during the adaptive process. The algorithm controls the edge error while respecting a fixed number of nodes in the mesh. From the latter, a threshold global error is computed and used to compute stretching and shrinking factors to adapt the mesh and move the existing nodes. In this work, instead, the interest is basically in adding new points to the existing mesh. Unlike the method in [33, 34], old mesh nodes will not be allowed to moved all over the domain. Therefore, as will be described in what follows, the algorithm will be adapted to a mesh node insertion approach.

### 3.2.2 Error criterion

The error criterion, called  $e_k$ , is quadratically defined on each edge  $k = 1, \dots, n_e$  as the projected gradient on that edge. Hence, the edge based error estimation is expressed as the following quantity:

$$e_k = \sqrt{\sum_{j=1}^{n_{dim}} \left( (g_j(\mathbf{x}_k^{(2)}) - g_j(\mathbf{x}_k^{(1)}))(x_{k_j}^{(2)} - x_{k_j}^{(1)}) \right)^2} \quad (21)$$

where  $\mathbf{x}_k^{(1)}$  and  $\mathbf{x}_k^{(2)}$  are the coordinates of the two nodes of a given edge, and  $g(\cdot)$  is the gradient of the function of interest. In practice, since the actual gradient usually is not known in this case, except for adjoint-based deterministic solvers, one could exploit the surrogate to compute numerical gradients at the training points.

The resulting algorithm is described in Algorithm 4. This procedure can then be repeated several times in an iterative cycle to increase sequentially the number of added training points.

---

#### Algorithm 4 Basic algorithm

---

- 1: Build the triangulation
  - 2: Compute  $e_k$  for each edge  $k = 1 \dots n_e$
  - 3: compute  $s_k = (\frac{e_{glob}}{e_k})^{1/2}$  and  $N(k) = \frac{1}{s(k)}$
  - 4: **for** each edge  $k$  **do**
  - 5:   **if**  $\lfloor N(k) \rfloor > 0$  **then**
  - 6:     add  $\lfloor N(k) \rfloor$  evenly spaced new points along the edge
  - 7:     add the new points to the DoE
  - 8:   **end if**
  - 9: **end for**
- 

In order to enrich the mesh construction approach, it is useful to add some information about the accuracy of the metamodel to the error estimator, since gradients are computed numerically starting from the metamodel itself. Therefore, it is interesting to refine also in regions where the gradient is low, if the metamodeling error is high, since it is not possible to trust completely the computed gradient value. Hence a weighted combination of Kriging variance and gradient error indicators can be developed.

A simple local-based error estimator for Kriging surrogate models is the Gaussian process variance. However, this indicator is zero at the training points, since the metamodel is an interpolation (in absence of nugget effect) and at these points we know the exact function value. A possible way to take it into account in the computation of the `edgeError(k)` is to consider its value  $\sigma_k = \sigma(\mathbf{x}_k^c)$  computed at the center of the edge  $\mathbf{x}_k^c = (\mathbf{x}_k^{(1)} + \mathbf{x}_k^{(2)})/2$ . Then it could be re-scaled and summed to the existing gradient based criteria  $e_k$ , defined in Eq. 21, as the following a weighted sum:

$$e_k^{\text{weighted}} = \alpha e_k + (1 - \alpha) \frac{\max_k (e_k)}{\max_k (\sigma_k)} \sigma_k \quad (22)$$

with the weight  $\alpha$  adjustable to control the relative influence of the two criteria.

### 3.2.3 Refinement by adding a fixed number of points

Having the possibility to add a fixed number of training points at each iteration of the adaptive process can be an advantage, because, in this way, it is easier for the user to parallelize, according to the available resources, the task of computing the actual value of the function of interest, which can involve expensive simulations. Two different strategies for the implementation of this feature are available. The first is a more rigorous mathematical formulation of the problem, but it translates in a more difficult and expensive solving algorithm, while the second tackles the problem directly with a faster algorithm. The two approaches are detailed in the following and named as *Brute Approach* and *Fast approach* (edge-based length distribution method), respectively.

The *Brute Approach* is a first rigorous attempt to node insertion. It consists in formulating the adaptation problem as finding the best combination of positions of a fixed number  $N_a$  of new nodes on the  $n_e$  edges in order to minimize an imposed error criterion. We seek to solve the following optimization problem:

$$N_k = \arg \min(\varphi(N_k)) \quad \text{with} \quad \varphi(N_k) = \sum_{k=1}^{n_e} \frac{1}{2} \frac{e_k}{(N_k + 1)^2} \quad (23)$$

$$\text{with the constraint: } N_a = \sum_{k=1}^{n_e} N_k$$

where  $e_k$  is the edge error and  $N_k$  is the number of nodes added for each edge. This optimization problem can be quite tricky to solve, due to the discrete nature of the design variables ( $N_k \in \mathbb{N}$ ). However, it can be noticed that, when  $N_a < n_e$ , it is possible to consider in the optimization just the  $N_a$  edges associated to a higher error value, so the problem becomes

$$N_k = \arg \min(\varphi(N_k)) \quad \text{with} \quad \varphi(N_k) = \sum_{k=1}^{N_a} \frac{1}{2} \frac{e_k}{(N_k + 1)^2} \quad (24)$$

$$\text{with the constraint: } N_a = \sum_{k=1}^{N_a} N_k$$

At this point, a possible approach to solve the problem through the use of brute force consists in seeking among all possible permutations of  $N_a$  nodes on  $N_a$

edges the one that minimizes  $\varphi(N_k)$ . As it can be easily detected, this approach is convenient just for small enough values of  $N_a$  (i.e.  $N_a \leq 10$ ), since the number of totalvi cases to be explored  $n_t$  increases quickly:

$$n_t = \frac{(N_a + N_a - 1)!}{(N_a - 1)!N_a!} \quad (25)$$

The method showed to be powerful and very accurate for low dimensions problems. However, it might be difficult to implement and expensive to solve for increasing size of the dimensional space.

The second approach, *i.e.* the *Fast approach*, consists in rewriting the optimization problem and modifying the iterative cycle of the original code in 3.2.1 so that it adds, at each iteration, a fixed number of points  $N_a$  imposed by the user. The implementation of the algorithm is described in Algorithm 5. While this insertion technique does not necessarily converge (from a strictly mathematical point of view), to the optimal rigorous solution, it highly decreases the computational cost, especially for higher values of  $N_a$ .

The nodes insertion method is adapted from the work in [33, 34] whereby an anisotropic mesh adaptation technique was introduced. The original method consists in computing a stretching factor associated with each edge in the mesh in the view of minimizing an error criterion over the mesh while respecting a certain fixed number of nodes. It starts by evaluating the edge based error estimates in terms of the gradient of the function under consideration. In this work, since the focus is only to insert new training nodes without moving the already existing points, an adaptation of the original algorithm is proposed.

The optimization problem can be stated also with respect to the stretching factors  $s_k$  associated to the edges of the mesh:

$$\begin{aligned} \text{minimize} \quad & \varphi(s_k) = \sum_{k=1}^{n_e} \frac{1}{2} s_k^2 e_k \\ \text{subject to} \quad & N_a = \sum_{k=1}^{n_e} \lfloor s_k^{-1} \rfloor \end{aligned} \quad (26)$$

since the number of points added on each edge can be related to the stretching factors (and hence to the error estimates) through the relation  $N_k = \lfloor s_k^{-1} \rfloor$ . An illustration of the node insertion approach along an edge  $\mathbf{C}^{ij}$  is illustrated in figure 2. It can be noticed, however, that also in this case, although the design variable is continuous, in the constraint there is a function that transforms it into an integer, and so the same difficulties present in the previous approach arise. In practice, this constraint is relaxed. Therefore, the strong formulation is replaced by a weak formulation defined by:

$$\begin{aligned} \text{minimize} \quad & \varphi(s_k) = \sum_{k=1}^{n_e} \frac{1}{2} s_k^2 e_k \\ \text{subject to} \quad & A = \sum_{k=1}^{n_e} s_k^{-1} \end{aligned} \quad (27)$$

where  $A = N_t + N_a$ , and  $N_t$  is the number of current training points. Then it

is possible to find a solution by using a Lagrangian formulation

$$\mathcal{L}(s_k, \lambda) = \frac{1}{2} \sum_{k=1}^{n_e} s_k^2 e_k + \lambda \left( \sum_{k=1}^{n_e} s_k^{-1} - A \right), \quad (28)$$

which leads to

$$s_k = \left( \frac{\lambda}{e_k} \right)^{\frac{1}{3}}, \quad (29)$$

with the multiplier

$$\lambda = \left[ \left( \sum_{k=1}^{n_e} e_k^{\frac{1}{3}} \right) / A \right]^3. \quad (30)$$

Clearly, the generated solution does not necessarily respect the exact number of nodes as a truncation to the integral part of  $s_k^{-1}$  is applied. This process adds new points where it is most needed i.e. where the error is most important. Hence the choice of considering the floor of  $s_k^{-1}$ . As a result, the solution of problem (27) results in an adaptation algorithm that adds a number of points close but not necessarily equal to  $N_a$  since the strong formulation is replaced by a weaker one. Therefore, in order to meet the fixed number of nodes, a correction part has been implemented in Algorithm 5. It consists in repeating the cycle of node insertion where the estimated error is most important as long as the target number of nodes has not been reached.

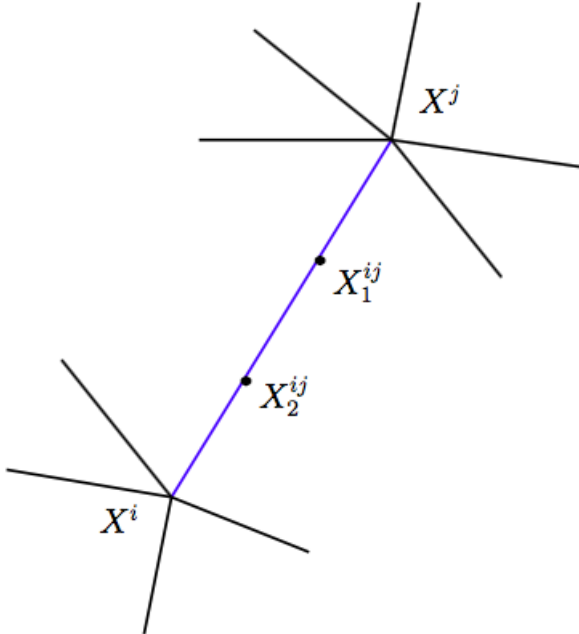


Figure 2: Adding  $\lfloor N(k) \rfloor = 2$  evenly spaced new points along the edge  $\mathbf{X}^{ij}$ , where  $k$  denotes the edge number.

### 3.2.4 Extrapolation technique for higher-dimensional input spaces

A drawback of the direct derivation of the adaptation methodology from the mesh adaptation technique is that, in order to be able to adapt in the whole domain, it is necessary to have nodes (training points) also in each vertex of the hypercube representing the domain when each input is uniformly distributed. However, this can be really limiting when the size of the input variables increases, since the number of vertices of the hypercube rapidly increases as  $2^{n_{dim}}$ , and subsequently the number of extra training points in which is necessary to evaluate the function of interest augments.

A possible simple solution for this problem, inspired by [26], can be to consider only training points inside the domain and then exploit an extrapolation to cover the remaining part up to the corners and the bounds. The extrapolation procedure can be structured as follows. First, a metamodel is trained on the initial design of experiments, which can be a normal Latin Hypercubes or quasi Monte Carlo design. Then the triangulation of the domain is built including also the corners in the set of nodes. It is important to mention that the true function values are not computed at these points. Thus, two different types of edges will be considered: the interpolation edges, constructed by joining two training nodes, and the extrapolation edges, for which at least one of the two nodes is a corner of the domain.

At this point, it is important to highlight the fact that since the actual value of the QoI is not known on the extrapolation edges, one could be less confident about the gradient value computed in the error criteria. Hence, when computing the global error, it is possible to put a smaller weight (or even a null weight) on the gradient part, with respect to the interpolation edges. Then the procedure for adding the new nodes is exactly the same as described in Algorithm 5. While the normal approach is supposed to work at least as fine, or even better, than the extrapolation one for smaller sizes of the input, this last should behave better when the number of input variables starts to increase, and the number of corners becomes comparable to the size of a DoE to get a sufficiently good metamodel of the QoI.

## 3.3 Parameters of interest

In this section, a brief overview is given on the parameters of the global algorithm that need to be set by the user, with their role and suggestions on a possible range of values.

Most of the parameters whose value needs to be imposed by the user are related to the sparse PDD algorithm. One of the most relevant is the maximum polynomial order  $m$ , since it strongly influences the accuracy of the intermediate sparse PDD metamodel, and hence the amount of information added to the final coupled metamodel. As it will be shown in Section 4.1, its value needs to be chosen according to the function of interest, and if necessary a preliminary test can be carried out. A bad value can spoil the convergence of the final metamodel. The value on  $\nu$ , the maximum size of ANOVA interaction terms, is easier to determine, as it can be left equal to the number of variables for smaller input, or fixed to 3 or 4 for higher inputs, following the principle that in most application cases, most relevant interactions occur at lower interaction orders. For the sensitivity of the sparse-PDD to the thresholds  $p$ ,  $\epsilon$ ,  $\theta$  and  $Q_{tgt}^2$  one can

Name	Possible values	Role
$m$	$[1, \infty]$	maximum polynomial degree for PDD
$\nu$	$[1, d]$	maximum size of ANOVA interaction
$p$	$[0, 1]$	variance threshold for adaptation in sparse-PDD
$\epsilon$ or $\theta$	$[0, 1]$	error threshold for adaptation in sparse-PDD
$Q_{tgt}^2$	$[0, 1]$	accuracy threshold for adaptation in sparse-PDD
$eglob$	$(0, \infty)$	error threshold in basic refinement algorithm
$N_a$	$[1, \infty]$	fixed number of added points in refinement algorithm
$i_{ref}$	$[0, \infty]$	number of iterations of the adaptation
$\alpha$	$[0, 1]$	error weight in refinement algorithm

Table 1: Parameters

refer to [15]. Author's experience would suggest to fix them to standard values and concentrate mostly on  $m$  to improve the convergence of the metamodel. Concerning the adaptation algorithm, the basic algorithm is not recommended in practical applications, since it is very hard to control the number of added points by changing the value of  $eglob$ . So the two main parameters that need to be assigned are the number of added points  $N_a$ , the number of iterations  $i$  and the error weight  $alpha$ . The normal operational use of the algorithm would be perform a small number of iterations, even just one, to add a number of nodes according to the available computational resources, if the accuracy of the metamodel trained on the initial experimental design is not satisfactory. A comparison of computations at different values of  $\alpha$  is proposed in Section 4.2.

## 4 Numerical experiments

In this section, several numerical experiments are presented. The objective is to illustrate performances and limits of the proposed approach, by making a systematic comparison with classical methods in literature.

Two classes of problems are used for validation purposes. First, some well-known algebraic functions, classically used in literature, are tested both without (in Section 4.1) and with mesh adaptation (in Section 4.2). Secondly, the method is tested on two engineering problems in aerospace application (Section 4.3). As it can be observed, the proposed method provides a systematic gain.

In Table 2 the characteristics of the test function used in the work are reported for clarity. Test 1 is a 2D function built with the purpose of testing the whole algorithm. Test 2, 3, 4 are well-known test functions for metamodels for UQ and optimization taken from literature.

Name	Input dim.	Domain	Function
TEST 1	2	$[-1, 1]$	$f(\mathbf{x}) = g(10x_1 - 2) \cos(5x_1^2) \cos(x_2^2)(3 - x_2)^2$ with $g(s) = \frac{s s }{1+s^2}$
TEST 2	3	$[-\pi, \pi]$	$f(\mathbf{x}) = \sin x_1 + a \sin^2 x_2 + bx_3^4 \sin x_1$
TEST 3	8	$[0, 1]$	$f(\mathbf{x}) = \prod_{i=1}^8 \frac{ 4x_i - 2  + c_i}{1 + c_i}$
TEST 4	100	$[0, 1]$	$f(\mathbf{x}) = \prod_{i=1}^{100} \frac{ 4x_i - 2  + c_i}{1 + c_i}$

Table 2: Test functions used for the assessment of the UK-PDD method



## 4.1 Results without mesh adaptation

The PDD-UK is used in this section to build metamodels for different test functions, verify the convergence of the metamodeling errors with the size of the Experimental Design and compare results with the ones obtained with Ordinary Kriging and sparse-PDD. Furthermore, the sensitivity of the method with respect to some parameters of the sparse adaptive selection of the PDD basis function is analyzed.

Along this section, Latin Hypercubes designs of different sizes are used as training points. Each training plan is used to build an Ordinary Kriging metamodel, a sparse-PDD one and a surrogate model exploiting the proposed PDD-UK method. The obtained surrogate models are tested on a LH plan of 100000 points.

### 4.1.1 TEST 1: 2D function

We introduce the following bivariate function (derived from an univariate test case already used in literature [40]):

$$f(\mathbf{x}) = g(10x_1 - 2) \cos(5x_1^2) \cos(x_2^2)(3 - x_2)^2 \quad \text{with} \quad g(s) = \frac{s|s|}{1 + s^2} \quad (31)$$

The function is evaluated in the domain  $\mathbf{x} \in [-1, 1]^2$ . It can be used as first simple case to test the convergence of the proposed method while increasing the size of the experimental design. The test is performed by increasing the number of training points, chosen by means of LH sampling. Note that the RMSE between the metamodels and the true function is computed on 100000 test points. Computations are repeated 15 times for each size of the DoE, in order to account for the variability of the experimental design. Results are reported in Figure 3. It can be seen that the RMSE of the coupled metamodel converges with the increasing of the number of training points and that its mean value is always lower than the ones of the two starting metamodels.

### 4.1.2 TEST 2: Ishigami function

The Ishigami function is another analytical example to verify the convergence of the method and to test the sensibility to some of the parameters. This function, which is widely used for benchmarking in global sensitivity analysis, depends on three independent input parameters and can be written as

$$f(\mathbf{x}) = \sin x_1 + a \sin^2 x_2 + bx_3^4 \sin x_1 \quad (32)$$

where the input random variables  $\mathbf{x} = \{x_1, x_2, x_3\}$  are uniformly distributed over  $[-\pi, \pi]$ . The constants are set to  $a = 7$  and  $b = 0.1$ , as done for example in [15, 13].

A maximum PDD order  $m = 3$  is initially considered and the two variance-based (v) and error-based (e) selection algorithms are compared. Table 3 reports values of RMSE,  $\text{MSE}_r$  and  $Q^2$  for all the surrogates. It can be noticed from this comparison that the variance-based adaptation approach for the sparse-PDD always produces a less accurate surrogate model with respect to the error based one. For this reason the set of basis functions given to the Universal

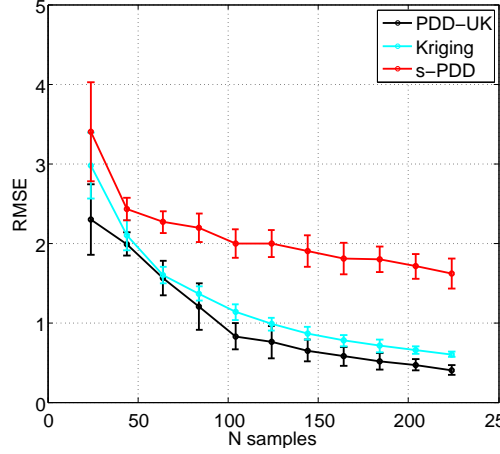


Figure 3: TEST 1: Mean RMSE convergence comparison between Ordinary Kriging, sparse PDD and coupled PDD-UK metamodelling,  $m = 5$

Kriging in the coupled approach, in the case of variance-based approach, is not enough representative of the function trends for the method to converge, hence no results are obtained. The error based approach, instead, is always able to produce a representative set of basis functions and the coupled method is then able to converge. When considering  $m = 3$  for the maximum PDD order, OK seems to perform better than sparse-PDD for the Ishigami function. Except for the 40 points training plan, the coupled method always delivers a better surrogate model (in the RMSE and  $Q^2$  sense) than the Ordinary Kriging and the sparse-PDD. This means that the added information in the regression part of the Kriging surrogate is actually able to improve the representation of the function, or, seen from the opposite point of view, that the Kriging departure term is able to improve the representation given only by the sparse-PDD regression. The exception in the 40 points training plan is likely caused by the fact that this set of points is too small to give enough information for the PDD to produce an accurate enough set of basis functions.

The same analysis is repeated when considering a higher maximum PDD order of  $m = 10$ . In Table 4, results are shown. When using the error-based adaptive approach, sparse-PDD surrogates are better than the Ordinary Kriging ones, and the coupled approach is always able to further reduce the metamodeling error. However, it is important to mention that, as pointed out in [15], the computational cost associated with the error-based criterion can be way higher than the one needed to perform the variance-based criterion because a higher number of terms is kept in the sparse representation. While this can be negligible for simple low-dimensional cases such as the Ishigami function, it can be relevant for higher-dimensional problems.

The comparison between the  $m = 3$  and the  $m = 10$  cases shows, as it could be expected, that this parameter has a high influence also on the quality of the final coupled metamodel, hence it must be chosen wisely. When no information is available about the choice of this parameter, a preliminary convergence study of the sparse-PDD algorithm can be performed at different values of  $m$  on the

$N_s$		OK	s-PDDe	PDD-UKe	s-PDDv	PDD-UKv
40	RMSE	2.19369	3.93583	3.14090	103.9839	-
	$MSE_r$	0.35438	1.09102	0.70760	1.0050	-
	$Q^2$	0.413350	0.534050	0.864321	-	-
80	RMSE	1.62157	2.92508	1.04595	74.7111	-
	$MSE_r$	0.19322	0.62815	8.0481e-2	1.00314	-
	$Q^2$	0.798325	0.527088	0.940881	-	-
160	RMSE	1.0656	2.53986	0.47179	7.54097	-
	$MSE_r$	8.27647e-2	0.47480	1.6393e-2	1.12117	-
	$Q^2$	0.897168	0.519746	0.973951	0.855120e-1	-
320	RMSE	0.66843	2.6088	0.34148	4.09612	-
	$MSE_r$	3.29050e-2	0.50122	8.58841e-3	0.79921	-
	$Q^2$	0.959829	0.633514	0.990904	0.572308	-
640	RMSE	0.442623	2.537008	0.227492	3.910519	0.369953
	$MSE_r$	1.442877e-2	0.474011	3.811484e-3	0.782575	1.007985e-2
	$Q^2$	0.981296	0.560523	0.995585	0.532891	0.986737

Table 3: TEST 2: Actual error measures for the Ordinary Kriging, Sparse-PDD with error-based (e) and variance-based (v) selection algorithms and coupled PDD-UK surrogate models of the Ishigami function,  $m = 3$ ,  $\theta = 10^{-5}$ ,  $\varepsilon_{Q^2} = 10^{-8}$ .

available design of experiments.

$N_s$		OK	s-PDDe	PDD-UKe	s-PDDv	PDD-UKv
40	RMSE	2.193697	3.68578	2.19369	-	-
	$MSE_r$	0.354380	1.00000	0.354380	-	-
	$Q^2$	0.413350	-	0.413350	-	-
80	RMSE	1.621572	1.08661	1.00083	50.22814	1.625250
	$MSE_r$	0.19322	8.69541e-2	7.376024e-2	1.30340	0.194121
	$Q^2$	0.798325	0.994236	0.995617	0.999215	0.792188
160	RMSE	1.06008	0.636108	0.35959	5.358411	1.0424
	$MSE_r$	8.2764e-2	2.9793e-2	9.5226e-3	2.114611	8.00259e-2
	$Q^2$	0.897168	0.995448	0.998263	0.999857	0.912285
320	RMSE	0.668438	0.32831	8.42948e-2	5.51245	0.63282
	$MSE_r$	3.2905e-2	7.93837e-3	5.233157e-4	2.23793	2.94929e-2
	$Q^2$	0.959829	0.998906	0.999896	0.999981	0.963671
640	RMSE	0.442623	7.291311e-2	1.559595e-2	5.161115	0.321574
	$MSE_r$	1.442877e-2	3.915368e-4	1.791371e-5	1.961754	7.615962e-3
	$Q^2$	0.981296	0.999900	0.999994	0.999978	0.989006

Table 4: TEST 2: Actual error measures for the Ordinary Kriging, Sparse-PDD with error-based (e) and variance-based (v) selection algorithms and coupled PDD-UK surrogate models of the Ishigami function,  $m = 10$ ,  $\theta = 10^{-5}$ ,  $\varepsilon_{Q^2} = 10^{-8}$ .

A further test of the convergence of the PDD-UK method can be performed on the sensitivity indices associated to the Ishigami function, since analytical values are known in literature (see for example [15]). A comparison with the numerical values obtained with the three metamodeling techniques under analysis and direct Monte Carlo sampling is reported in Table 5. In a practical application the MC approach would be drastically more expensive than the others, due to the high number of model evaluations required, hence the metamodel-based techniques represent a very good trade off between accuracy and efficiency. A

general good convergence is shown for the first order sensitivity indices, while the convergence of the second order indices is more difficult for the Monte Carlo based computations, especially when they have really small (or null) values. This is an intrinsic characteristic of the Monte Carlo computation of the indices, since high order indices computation depends also on the computed values of lower order indices [16], and so it can be spoiled by a loss of accuracy (see for example the negative index in Tab. 5). Hence, the sparse-PDD technique seems to be more suited if the only purpose is the sensitivity analysis, because, due to its close link with ANOVA decomposition, the computation of the indices is straightforward and more accurate, especially for higher order ones. However, as seen before, the UK-PDD metamodel has a lower cross-validation error if the PDD basis is enough representative. Furthermore, another advantage of the PDD-UK metamodel over the sparse-PDD is that, being a Gaussian process metamodel, it can be exploited in several optimization applications, in combination with techniques such as the Expected Improvement and EGO algorithm [41].

SI	Exact	Kriging	s-PDDv	PDD-UKv	s-PDDe	PDD-UKe	MC
$S_1$	0.3138	0.3558	0.3133	0.3486	0.3126	0.3137	0.3147
$S_2$	0.4424	0.4804	0.4397	0.4949	0.4448	0.4431	0.4419
$S_3$	0	0.0063	0	0.0064	0	0.0046	0.0045
$S_{12}$	0	0.0053	0	0.0035	0	-0.0002	0
$S_{13}$	0.2436	0.1462	0.2470	0.1426	0.2423	0.2386	0.2389
$S_{23}$	0	0.0031	0	0.0022	0	0.0001	0
$S_{123}$	0	0.0029	0	0.0018	0.0023	0.0001	0
$f_0$	3.5	3.4861	3.5023	3.4785	3.4983	3.4946	3.4955
$D$	13.845	11.8388	13.9338	12.7512	13.8550	13.8793	13.8720
$Q^2$		0.91604	0.99959	0.92383	0.99991	0.99996	
eval.		200	200	200	200	200	100000

Table 5: TEST 2: numerical mean, variance, metamodel accuracy and sensitivity indices of the Ishigami function obtained with different metamodeling techniques and comparison with exact and Monte Carlo results,  $m = 10$ ,  $\nu = 3$ ,  $\varepsilon_{Q^2} = 10^{-8}$ ,  $\theta = 10^{-3}$ .

#### 4.1.3 TEST 3: 8D Sobol function

To test the approach on a higher-dimensional problem, the eight-dimensional Sobol function test case is considered [15]. Its expression is:

$$f(\mathbf{x}) = \prod_{i=1}^8 \frac{|4x_i - 2| + c_i}{1 + c_i} \quad (33)$$

where the components of the input vector  $\mathbf{x}$  are uniformly distributed over  $[0, 1]$  and the vector of positive coefficients is  $\mathbf{c} = \{1, 2, 5, 10, 20, 50, 100, 500\}$ .

A first comparison between Ordinary Kriging, sparse PDD and the coupled PDD-UK method can be performed on the first order sensitivity indices obtained with the three surrogate modeling techniques. Results are reported in Table 6, and a further comparison is done with analytical (exact) results and values obtained with a classical Monte Carlo sapling performed on the original function. Results show a general good convergence of all methods. It can be noticed that,

while being slightly more accurate in some cases, especially for the most influent indices, the coupled PDD-UK approach is not able to outperform the sparse-PDD in the approximation of the sensitivity indices, as observed also for the Ishigami function. Hence, in general, it could be not necessary to perform the MC sampling on the final UK-PDD surrogate to obtain the SIs, but one could simply rely on the use of the PDD coefficients computed during the intermediate construction of the sparse-PDD surrogate. In this way the SIs would come almost effortlessly and with a good accuracy.

SI	Exact	Kriging (MC)	s-PDD	PDD-UK (MC)	MC
$S_1$	0.603	0.654	0.632	0.607	0.603
$S_2$	0.268	0.265	0.284	0.269	0.271
$S_3$	0.067	0.045	0.048	0.072	0.069
$S_4$	0.020	0.015	0.018	0.025	0.022
$S_5$	0.0055	0.004	0.006	0.010	0.009
$S_6$	0.000	0.002	0.002	0.005	0.003
$S_7$	0.000	0.002	0.003	0.004	0.003
$S_8$	0.000	0.001	0.003	0.004	0.002
$f_0$	1.0000	1.0064	0.9988	0.9960	0.9998
$D$	0.1380	0.1185	0.1307	0.1302	0.1378
$Q^2$		0.9394	0.9896	0.9913	
model evaluations		150	150	150	100000

Table 6: TEST 3: numerical mean, variance, metamodel accuracy and sensitivity indices of the 8-dimensional Sobol function obtained with different metamodeling techniques and comparison with exact and Monte Carlo results,  $m = 4$ ,  $\nu = 2$ .

A second convergence test can be performed by plotting the trends of the RMSE and  $Q^2$  when increasing the size of the training plan  $N_s$  at different values of the maximum polynomial degree  $m$ . Values are compared for both the simple sparse-PDD method, the Ordinary Kriging and the couple UK-PDD method. Results are shown in Figure 4. The comparison shows that the convergence of the sparse-PDD is not monotone with the value of  $m$ , as already remarked in [15], and this reflects on the convergence of the coupled method. In this context, the more complex and expensive coupling strategy developed in [13] could reduce the sensitivity of the final PDD-UK metamodel to the maximum polynomial order  $m$ , but with an increasing computational effort, which could not be justified, as in general all the coupled metamodels at different values of  $m$  are better than the single sparse-PDD ones (in the RMSE sense). Another aspect that is important to notice is that the  $Q^2$ , and so the cross-validation error, sometimes are not able to capture properly the difference in accuracy of different metamodels, especially when they are relatively close. This is a known fact, which must be kept into account in application where is not possible to compute the RMSE.

#### 4.1.4 TEST 4: 100D Sobol function

A high-dimensional test case is proposed here with the 100-dimensional Sobol function. The model is the same as in the previous case 4.1.3, but with different parameter values, namely  $c_i = i^2$ . This means that the influence of the variables on the output decays quite rapidly with their index. For this high-dimensional

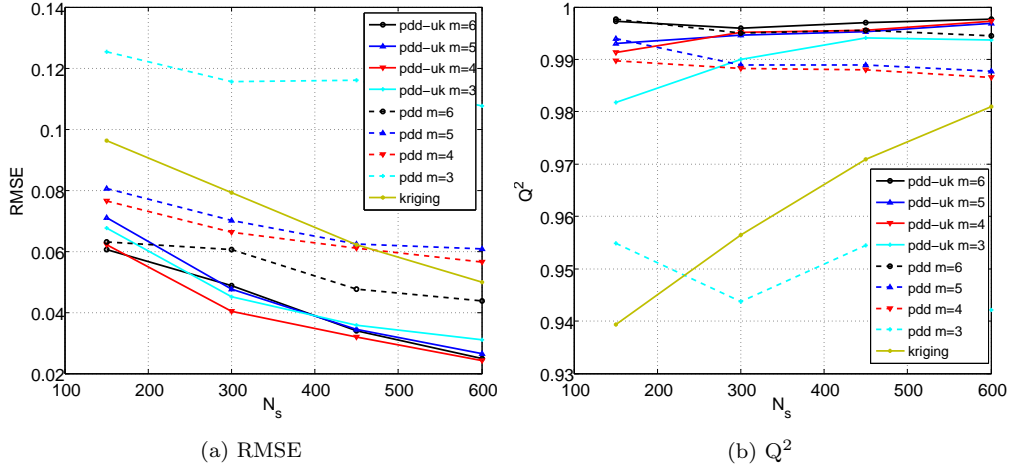


Figure 4: TEST 3: Actual (RMSE) and cross-validation ( $Q^2$ ) error measures when increasing the number of training points. Results are plotted for the Ordinary Kriging, Sparse-PDD and coupled PDD-UK surrogate models of the 8-dimensional Sobol function at different values of  $m$ . Error-based adaptive algorithm.

test case, the error-based algorithm is computationally too expensive, so computations are performed only with the variance-based selection algorithm. A convergence study is performed by gradually increasing the number of Latin Hypercubes training points. The maximum polynomial order  $m$  is fixed to 4, since, as pointed out in [15], for  $m = 3$  the accuracy of the metamodel for the sparse PDD tends to decrease when increasing the size of the design of experiments, and some preliminary tests showed that the coupled approach was not always able to produce good results in this case.

In Figure 5, errors estimates are reported for the three metamodeling methods at different sizes of the DoE. First of all, it has to be noticed that the error associated to the Ordinary Kriging is quite large, as the number of training points used is quite limited with respect to the number of input variables, and in general it is not easy to build an accurate Ordinary Kriging surrogate model with a high-dimensional input. However the sparse PDD is able to produce far better results, since the adaptive procedure allows to recognize the most influencing variables and neglect the others. The coupled approach is able to exploit the sparse functional basis taken from the sPDD and so that also its metamodeling error is relatively small.

Note that the RMSE associated to both the sPDD and the PDD-UK decreases when increasing the number of training points, while the cross-validation error increases slightly. As observed in [15], the  $Q^2$  error estimate could not always be the most appropriate way to compare metamodels accuracy, since it directly depends on the design of experiments and its size. Unfortunately, when the computation of the RMSE is unaffordable, one must rely on some error estimate as the GCV, to state the accuracy of the surrogate.

Finally, in Table 7 a comparison is proposed for the bigger Experimental

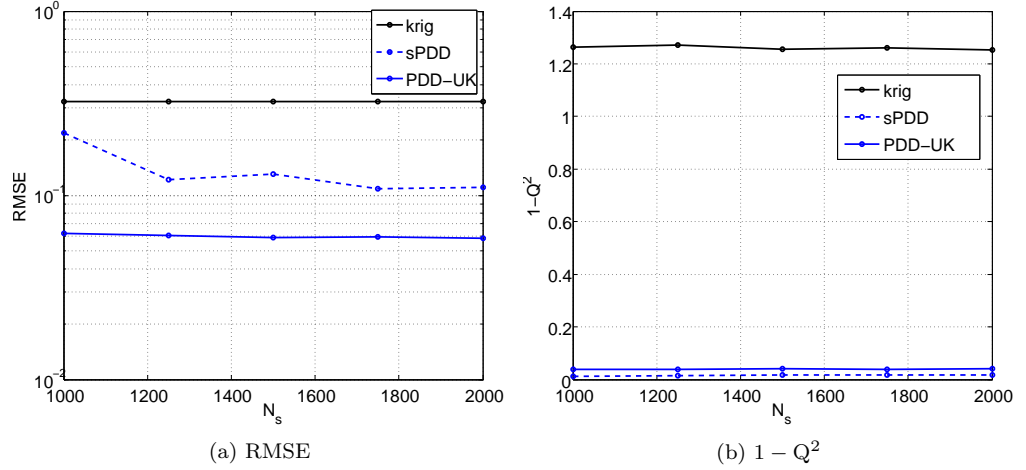


Figure 5: TEST 4: Actual (RMSE) and cross-validation ( $1 - Q^2$ ) error measures when increasing the number of training points. Results are plotted for the Ordinary Kriging, Sparse-PDD and coupled PDD-UK surrogate models of the 100-dimensional Sobol function. Variance-based adaptive algorithm.

Design between the RMSEs of the three metamodels (as in figure 5b) with the addition of the RMSE of a PDD-UK surrogate built only on the variables that have a positive contribution to the output variance computed in the sparse-PDD adaptation process, which for this case are only 24 over 100. It is possible to notice that this leads to a further improvement of the metamodeling accuracy, with a further reduction of RMSE.

Kriging	s-PDD	PDD-UK	PDD-UK reduced
0.3229	0.11021	5.8727E-002	1.7138E-002

Table 7: TEST 4: comparison of RMSE between ordinary Kriging, spare PDD, PDD-UK and PDD-UK with reduction of the input dimension, 2000 training points.

## 4.2 Assessment of the adaptive strategy

In this section, the proposed strategy to adaptively add new points to the Experimental Design is assessed. Firstly, the fast approach is compared to the more rigorous one to verify its robustness. Then, several iterations of the adaptation algorithm are applied to different test functions to test its convergence in RMSE sense. It has to be noticed that in a normal application, just few iterations of the algorithm are likely to be performed, since, if the adequate computational power is available to evaluate the QoI in several training points, it would be more advisable to generate a larger Experimental Design from the beginning.

#### 4.2.1 Comparison between brute and fast approach

First, we present here a comparison between the optimal but computationally expensive approach and the faster one (see Sec. 3.2.3). The analysis is performed on the TEST 1 function (see Table 2).

In Figure 6, results obtained starting from an initial LHS design of 24 points (20 actual LHS points plus the four corners of the bidimensional domain) are compared. Comparisons between the brute (a,c,e) and the faster approach (b,d,f) are performed for three different values of  $\alpha$ , *i.e.* 0.2, 0.5 and 0.8. Note that curves relative to different values of  $N_a$  are shown in different colors. As it is possible to notice, the obtained solutions are, most of the times, practically identical between the two algorithms for both different values of the parameters  $N_a$  and  $\alpha$ . Sometimes, as it can be seen in Figure 6b for  $N_a = 2$ , the convergence of the faster algorithm is even better. Concerning the computational cost of the two algorithms, figure 7 shows the trend of the CPU time when increasing the number of points added at each iteration, *i.e.*  $N_a$ , for different values of  $\alpha$ . It can be seen that, as expected, the fast algorithm outperforms the brute approach for  $N_a > 10$ . In fact, the brute approach becomes almost infeasible in this conditions. Note also that, for the fast algorithm, the computational time decreases with  $N_a$ , because less iterations of the adaptation algorithm are required, which includes also the construction of the Delaunay triangulation of the domain. This difference in computational cost is expected to increase with the size of the input space.

The same convergence analysis can be repeated for a larger training plan, this time of 44 training points. The behavior, as shown in Figure 8, is generally the same, with the fast algorithm performing at least as good as the other one.

#### 4.2.2 Convergence

As stated in the previous section, the fast algorithm is able to perform adequately well and allows a bigger flexibility and lower computational cost with respect to the so-called brute approach. Using this assumption, the fast algorithm is then retained for the following analysis. The adaptive part of the algorithm is then tested on TEST 1, 2 and 3 (see Table 2).

First, we assess the convergence of the algorithm for the TEST 1 function. The convergence is assessed by repeating the adaptation process starting from fifteen different LH designs of same size, and comparing then the obtained RMSE mean value and the standard deviation with the ones one would get with standard LHS designs of increasing size. In Figure 9, it can be seen that, for this test case, the mean error related to the adaptive strategy converges faster than the one of a simple LHS, especially for  $\alpha = 0.5$  and  $\alpha = 0.2$ , namely when taking into account also the Kriging estimation of the metamodeling error. Furthermore, the adaptation in this particular test case delivers more robust results, since variance of the RMSE is smaller.

Concerning the TEST 2 function (see Table 2), Figure 10 shows that the adaptive strategy converges faster than the simple LHS, especially for  $\alpha = 0.5$  and  $\alpha = 0.2$ . It also shows that adding a relatively higher number of training points per iteration helps keeping the convergence curve more stable.

Finally, a test is performed on the TEST 3 function introduced in Table 2,



to verify if convergence is retained also on a higher-dimensional case. Results for this test are reported in Figure 11 and 12. As it can be seen in 11a, the normal approach does not show to converge at least as fast as LHS, probably due to the fact that a relatively high number of training points with respect to the size of the initial DoE (256 over 320) needs to be put in the corners of the domain, leaving too little information to train an adequate metamodel inside the domain. Therefore, the adaptation is repeated with the extrapolating approach in Figure 11b, where all the training points are strictly inside the domain, which is able to improve results and to provide a convergence which is, for the first iteration, much better than the one obtained by just increasing in the size of the LHS plan. This extrapolating approach also allows to reduce the number of training point to a number which is lower than (or very close to) the number of corners, as shown in Figure 12. It can be however noticed that the convergence of the adaptive approach for this 8-dimensional case tends rapidly to be almost flat when adding 100 new points for each iteration. It is noticeable instead (Figure 12b), when adding 50 samples per iteration, that the metamodeling error decreases generally faster than with the normal LHS: the first iteration decreases strongly the error, and while next iteration tend to realign to LHS, the trend is however better.

### 4.3 Engineering Applications

The proposed method is then tested on two different applications in the aerospace field. For these cases, one evaluation of the quantity of interest corresponds to the output of a computer code describing the specific physics of interest.

#### 4.3.1 EXPERT reentry

The engineering application firstly proposed is in the context of the hypersonic flow that occurs during the entry trajectory of the EXPERT space vehicle by the European Space Agency. The goal is the construction of a metamodel for the stagnation pressure  $p_{st}$ , which is one of the quantities measured by the sensors flush-mounted in the nose of the vehicle, as function of the freestream values and some chemistry parameters described next [42]. Two points in the entry trajectory of the vehicle are investigated. For each point, nominal freestream conditions are described in table 8. The trajectory point at higher altitudes is known to exhibit chemical non-equilibrium effects in the shock layer, while in the lower point of the trajectory, which is close to the peak heating conditions, the chemistry is mainly in equilibrium.

Altitude, Km	$T_\infty$ , K	$p_\infty$ , Pa	$M_\infty$
60	245.5	20.3	15.5
30	220	1200	12.3

Table 8: Freestream conditions for the entry trajectory points of the EXPERT vehicle.

The set of equations used to describe the phenomena is a combined physico-chemical model, developed by Barbante [43], able to simulate hypersonic high-

temperature reacting flows. Two-dimensional axisymmetric Navier-Stokes equations, supplied with adequate boundary conditions, are combined with the chemical mechanism introduced by Park et al. [44] applied to a mixture of five species air (N, O, NO, N<sub>2</sub> and O<sub>2</sub>). Furthermore, the catalyticity of the vehicle surface is taken into account, and it is modeled as a catalytic wall at radiative equilibrium. To simulate the forward problem, we use the in-house code COSMIC developed by Barbante [43]. This solver was designed to approximate hypersonic flow models where chemical non-equilibrium effects need to be accounted for. It includes a hybrid upwind splitting scheme, the hybridization of the van Leer scheme [45] and the Osher scheme [46] and adds a carbuncle fix. An axisymmetric condition is imposed on the symmetry axis, while the wall of the body is modeled by a partially catalytic wall at radiative equilibrium. An example of the solution temperature field for the nominal conditions at 60km altitude is shown in Figure 13.

Concerning the uncertainty characterization of the input, the unknown freestream pressure and Mach number  $p_\infty$ ,  $M_\infty$  are assumed to follow uninformative uniform distributions, and uniform epistemic uncertainty is associated also to the catalytic recombination coefficient  $\gamma$ , as described in Table 9. Uncertainty is taken into account also on four reactions rates  $k_r$  of four chemical dissociation processes, and they are assumed distributed with log-normal distributions (see Table 10).

Variable	Distribution	Minimum	Maximum
$p_\infty$ [Pa]	Uniform	16.3	24.3
$M_\infty$	Uniform	13.7	17.3
$\gamma$	Uniform	0.001	0.002

Table 9: Uncertainties on freestream conditions and catalytic recombination constant.

Gas reaction	Distribution of $\log_{10} k_r$	$\sigma_r$
$\text{NO} + \text{O} \rightarrow \text{N} + \text{O} + \text{O}$	Normal	0.12
$\text{NO} + \text{N} \rightarrow \text{N} + \text{O} + \text{N}$	Normal	0.12
$\text{O}_2 + \text{N}_2 \rightarrow 2\text{O} + \text{N}_2$	Normal	0.10
$\text{O}_2 + \text{O} \rightarrow 2\text{O} + \text{O}$	Normal	0.10

Table 10: Uncertainties on gas reaction rates.

In Tables 11 and 12, RMSEs are compared to assess the quality of the different surrogate models for two different points of the trajectory. Three different Latin Hypercubes designs of experiments of increasing size (respectively 120, 680 and 3060 points) are utilized, to state the convergence of the combined method and to verify the gain in efficiency with respect to the other two techniques.

It can be seen that, for both trajectory point, the metamodeling error associate to the stagnation pressure is lower for the PDD-UK surrogate. This happens because the PDD method is well converged and so the selected basis function are able to add useful information to the Universal Kriging. The weak

$N_s$	OK	s-PDD	PDD-UK
120	4538.72	1252.28	364.44
680	2275.62	1134.35	188.77
3060	806.349	1068.32	114.88

Table 11: EXPERT reentry, 30km point, RMSE comparison of the metamodels for the stagnation pressure,  $\nu = 2$ ,  $m = 4$ ,  $\varepsilon_{Q^2} = 10^{-7}$ .

$N_s$	OK	s-PDD	PDD-UK
120	50.577	23.563	19.945
680	14.918	20.458	13.875
3060	11.095	19.541	10.993

Table 12: EXPERT reentry, 60km point, RMSE comparison of the metamodels for the stagnation pressure,  $\nu = 2$ ,  $m = 4$ ,  $\varepsilon_{Q^2} = 10^{-7}$ .

point in the training algorithm appears to be good choice of the s-PDD parameters and in general the convergence of this part of the metamodel. When a good PDD metamodel is trained, often the coupled method has a lower RMSE than both simple techniques, otherwise it can be worse than one of them. The Ordinary Kriging seems instead the more robust of the the three algorithms, once the hyperparameters are correctly optimized.

#### 4.3.2 TACOT ablation test case

A higher dimensional engineering case is here proposed with the analysis of the temperature of an ablative material at a fixed position and imposed time of an ablation process. In particular, let us consider the unidirectional ablation of a 7.21cm thick TACOT (Theoretical Ablative Composite for Open Testing) material, exposed to a constant heat flux for one minute before radiatively cooling down. This rectangular incoming flux, is an interesting case to test the method proposed in this paper. While this case does not represent the atmospheric entry of a spacecraft, it is however quite close to an ablation test in the Plasmatron facility [47].

Uncertainties are considered on 27 input parameters related to the physical and chemical properties of the material. An uniform distribution is associated to each uncertain variable, with values reported in Table 13. The quantity of interest is the temperature of the material at a position of  $x = 5.61\text{cm}$ , meaning 1.6cm from the heated surface, at the time  $t = 80\text{s}$  over 120s of simulation (see Figure 14), performed with the PATO code [48]. In order to reduce the computational effort while not affecting the metamodeling accuracy, the PDD-UK is built just on the input variables which are not completely neglected in the the sparse-PDD regression, as tested on the 100-dimensional Sobol function in Sec. 4.1.4. This leads to considering only 18 input dimensions in the final metamodel.

The comparison between the three metamodeling techniques is reported in Table 14. First of all, it can be noticed that each one of the three techniques shows to converge when increasing the size of the Latin Hypercubes Experimen-

Variable	Description	Minimum	Maximum
$\rho_f$	Fiber density	1520	1680
$\epsilon_f$	Fiber volume fraction	0.095	0.105
$\rho_m$	Matrix density	1140	1260
$\epsilon_m$	Matrix volume fraction	0.095	0.105
$K_v$	Permeability of the virgin material	1.52e-11	1.68e-11
$K_c$	Permeability of the char	1.9e-11	2.1e-11
C	Carbon fraction	0.1854	0.2266
H	Hydrogen fraction	0.6111	0.7469
O	Oxygen fraction	0.1035	0.1265
$A_1$	Pre-exponential factor reaction 1	10800	13200
$e_1$	Activation energy reaction 1	64017.801	78243.979
$h_1$	Pyrolysis enthalpy reaction 1	-4.4e6	-3.6e6
$A_2$	Pre-exponential factor reaction 2	4.479993e8	5.475547e8
$e_2$	Activation energy reaction 2	1.529775e5	1.869725e5
$h_2$	Pyrolysis enthalpy reaction 2	-4.4e6	-3.6e6
$c_p$	Heat capacity virgin	0.95	1.05
$k_i$	Conductivity i virgin	0.95	1.05
$k_j$	Conductivity j virgin	0.95	1.05
$k_k$	Conductivity k virgin	0.95	1.05
$C_e$	Emissivity virgin	0.95	1.05
$C_r$	Reflectivity virgin	0.95	1.05
$c_p$	Heat capacity char	0.95	1.05
$k_i$	Conductivity i char	0.95	1.05
$k_j$	Conductivity j char	0.95	1.05
$k_k$	Conductivity k char	0.95	1.05
$C_e$	Emissivity char	0.95	1.05
$C_r$	Reflectivity char	0.95	1.05

Table 13: Uncertainties characterization for PATO: minimum and maximum of the uniform distribution associated to each uncertain input.

tal Design. For the smaller design with size of 200 samples, the best performing surrogate is Ordinary Kriging. Since more than 100 basis functions are kept in sparse PDD representation with  $\nu = 2$ ,  $m = 4$ , the computation of the coefficients and so the choice of the rejected basis function can not be accurate enough for the smaller designs, hence also the coupled PDD-UK metamodel suffers the inaccurate choice of regression functions, and results less accurate than Ordinary Kriging. However, when enough training points are considered, the metamodeling error of the PDD-UK becomes the smaller of the three techniques. The convergence of the method for smaller DoE could be improved by reducing the number of terms kept in the final regression by reducing the maximum polynomial order and the order of interaction, as shown in the case 2, with  $\nu = 1$ ,  $m = 2$ . The RMSE values obtained for optimized values of  $\nu$  and  $m$  parameters is reported in table 15. The maximum ANOVA interaction is set  $\nu = 2$ , and  $m$  is kept equal to one for the smaller training plans and then increased to two at 700 training points. Note the consistent gain in accuracy obtained with the coupled metamodel for smaller experimental design, while for the bigger the error seems to be at convergence.

$N_s$	OK	s-PDD 1	PDD-UK 1	s-PDD 2	PDD-UK 2
200	2.4191	3.8836	3.8798	2.9348	2.5952
300	1.5707	3.3070	2.7257	2.6766	1.4420
400	1.2439	3.0733	1.8667	2.6449	1.1829
500	0.9394	1.9956	0.6890	2.6574	0.8736
600	0.7055	1.6047	0.4821	2.5490	0.6620
700	0.5779	1.3625	0.4470	2.5658	0.5427

Table 14: PATO, RMSE comparison of the metamodels,  $\nu = 2$ ,  $m = 4$  for case 1,  $\nu = 1$ ,  $m = 2$  for case 2.

$N_s$	OK	s-PDD	PDD-UK
200	2.4191	2.4103	1.6193
300	1.5707	2.2190	0.8193
400	1.2439	1.8097	0.5365
500	0.9394	1.4698	0.4777
600	0.7055	1.3344	0.4235
700	0.5779	1.1882	0.4232

Table 15: PATO, RMSE comparison of the ordinary Kriging, sparse-PDD and PDD-UK metamodels, with optimized parameter  $m$  for the PDD at each training set. A value of  $\nu = 2$  have been used.

## 5 Conclusions

This paper proposed a framework for the training of an efficient metamodel for cases when expensive numerical simulations are required to evaluate the functions of interest. The global strategy have been described.

A coupled metamodeling approach has been proposed, consisting in the use of sparse polynomials selected by sparse Polynomial Dimensional Decomposition as basis functions for the regression term of Universal Kriging surrogate model. This improves the convergence of the metamodel with respect to both Ordinary Kriging and Polynomial Dimensional Decomposition, as tested on different test cases.

An algorithm to adaptively enrich the set of training points has also been proposed. It relies on the construction of a  $n$ -dimensional Delaunay grid in the space of the input variables, using the sampling points as nodes of the grid, and then in the application of an adaptation algorithm derived from mesh adaptation techniques. It consist in adding point to minimize an error measure that balances the estimate of the metamodeling error with the function gradients. The convergence of this techniques has been tested on different test functions with input space up to 8-dimensions. The algorithm shows to perform better than the simple use of a more refined Latin Hypercube sample, especially for the lower dimensional test cases and when considering just one adaptation iteration to add a few points to an already meaningful experimental design.

Finally, the coupled metamodel has been tested with good results on two medium-to-high-dimensional engineering applications in the aerospace context. The first one, taking into account 7 uncertain inputs, consisted in the training of

a metamodel for the stagnation pressure of the hypersonic entry flow around the nose of the EXPERT vehicle. The second was the construction of a metamodel for the temperature in a fixed point of an ablating material, as a function of 27 input parameters.

## A Metamodel assessment

Several error measures can be found in literature to state the quality of the metamodel, that is its local or global difference with respect to the actual function of interest. In this paper, different techniques are used, for sake of comparison with previous works. Here can be found a definition of the used error measures.

If one can afford to compute the actual value of the quantity of interest in different points of the stochastic space other than the training points, it is easy then to compute the difference at those points between the actual solution and the prediction given by the surrogate. Then it is possible to integrate this local error to obtain the actual global root mean squared error (RMSE). In practice the integration is done by a numerical integration technique [49]:

$$\text{RMSE} = \sqrt{\frac{1}{N_t} \sum_{i=1}^{N_t} (f(\mathbf{x}_i) - \hat{f}(\mathbf{x}_i))^2} \quad (34)$$

The same information can be used to compute a normalized measure called relative mean square error  $\text{MSE}_r$  [13]:

$$\text{MSE}_r = \frac{\sum_{i=1}^{N_t} (f(\mathbf{x}_i) - \hat{f}(\mathbf{x}_i))^2}{\sum_{i=1}^{N_t} (f(\mathbf{x}_i) - \hat{\mu}_y)^2} \quad (35)$$

where  $\hat{\mu}_y$  is the estimated mean of the output variable.

Often, in practical applications the computational cost associated to the evaluation of the model solution is too high, hence the RMSE can not be directly computed. In this cases an estimate of the error measure is instead required. One of the most common global error estimate in literature is *leave-one-out cross validation* (CV) [50, 49]. It consists in fitting the Kriging surrogate model on  $N_s - 1$  points, by leaving out one training point at a time, then the response is predicted at this point with the metamodel. Then the CV error can be defined as

$$\text{CV} = \sqrt{\frac{1}{N_s} \sum_{i=1}^{N_s} (f_i - \hat{f}_i^{(-i)})^2} \quad (36)$$

where  $f_i$  is the training point observed response, while  $\hat{f}_i^{(-i)}$  is the prediction at the left-out point using the surrogate built from all the other points. An easier interpretation of the CV error can be achieved by computing the determination coefficient  $Q^2$

$$Q^2 = 1 - \frac{\text{CV}^2}{\hat{V}[\mathcal{Y}]} \quad (37)$$

where

$$\hat{V}[\mathcal{Y}] = \frac{1}{N_s - 1} \sum_{i=1}^{N_s} (y_i - \bar{y})^2 \quad \text{with} \quad \bar{y} = \frac{1}{N_s} \sum_{i=1}^{N_s} y_i \quad (38)$$

Hence if  $Q^2$  is close to unity it means that the metamodel is able to well fit the function of interest.

## B Sensitivity Indices

Let us briefly recall the ANOVA representation of a multivariate function:

$$y = f(\mathbf{x}) = f_0 + \sum_{s=1}^N \sum_{i_1 < \dots < i_s}^N f_{i_1 \dots i_s}(x_{i_1}, \dots, x_{i_s}) \quad (39)$$

Since the members in Eq. 2 are orthogonal, the contribution of a subset of variables to the variance is

$$D_{i_1 \dots i_s} = \int f_{i_1 \dots i_s}^2 dx_{i_1} \dots dx_{i_s} \quad (40)$$

and if  $D$  is the global variance of  $f$ , it is clear that from the ANOVA expansion follows that

$$D = \sum_{s=1}^N \sum_{i_1 < \dots < i_s}^N D_{i_1 \dots i_s}. \quad (41)$$

The global sensitivity indices (SI), which estimate the influence of a single variable or a group of variables on the global model output, can be defined as:

$$S_{i_1 \dots i_s} = \frac{D_{i_1 \dots i_s}}{D} \quad (42)$$

From this definition, it is possible to see that all the  $S_{i_1 \dots i_s}$  are non negative and that they sum up to the unity:

$$\sum_{s=1}^N \sum_{i_1 < \dots < i_s}^N S_{i_1 \dots i_s} = 1 \quad (43)$$

The evaluation of the integrals involved in the computation of the sensitivity indices can be performed with a Monte Carlo (MC) or quasi-Monte Carlo (qMC) techniques, following the approach proposed by Sobol' in [17]. The drawback of this method is that its convergence is quite slow, thus requiring several thousands of evaluations of the quantity of interest. While this approach could be impossible to be adopted directly on the expensive forward model of a complex simulation, it could be accelerated by the use of the Kriging surrogate model.

## Acknowledgments

Andrea F. Cortesi has been supported by DGA (Direction Générale de l'Armement) from French Government. This material is based on work supported by Department of Defense, Defense Advanced Research Project Agency's program Enabling Quantification of Uncertainty in Physical Systems. The second author's work is partially supported by (i) DARPA's Enabling Quantification of Uncertainty in Physical Systems (EQUIPS) program and (ii) U.S. Department of Energy Office of Science, Office of Advanced Scientific Computing Research, Applied Mathematics program under Award Number DE-SC- 0011077. Authors wish to thank Georgios Bellas-Chatzigeorgis and Paolo Barbante for their support with regard to numerical simulations with the COSMIC code.

**Algorithm 5** Fixed  $N_a$  adaptation, fast approach

---

```

1: Calculate  $e_k$  for each  $k = 1, \dots, n_e$ 
2: Compute  $\lambda = (\sum_{k=1}^{n_e} \frac{e_k^{1/3}}{A})^3$ , where  $A = N + N_a$ 
   and  $s_k = (\frac{\lambda}{e_k})^{1/3}$ 
3: Compute  $N_k = \lfloor \frac{1}{s_k} \rfloor$ 
4: while  $k \leq n_{edges}$  and  $\sum_k n_p < N_a$  do
5:   if  $(N_k > 0)$  then
6:     for  $j = 1 : N_k$  do
7:        $n_{p_k} = n_{p_k} + 1$ 
8:       if  $\sum_i n_p = N_a$  then
9:         EXIT
10:      end if
11:    end for
12:  end if
13:   $i = i + 1$ 
14: end while
15: if  $\sum_i n_p < N_a$  then
16:   Compute  $s_k^{new} = \frac{1}{s_k} - N_k$ 
17:   Sort the edges  $k$  according to their value of  $s_k^{new}$  in decreasing order and
   compute  $N_k^{new} = \lfloor \frac{1}{s_k^{new}} \rfloor + 1$ 
18:   while  $k \leq n_{edges}$  and  $\sum_k n_p < N_a$  do
19:     if  $(N_k^{new} > 0)$  then
20:       for  $j = 1 : N_k + 1$  do
21:          $n_{p_k} = n_{p_k} + 1$ 
22:         if  $\sum_i n_p = N_a$  then
23:           EXIT
24:         end if
25:       end for
26:     end if
27:      $k = k + 1$ 
28:   end while
29: end if
30: for each edge  $k$  where  $n_{p_k} > 0$  do
31:   add  $n_{p_k}$  evenly spaced new points along the edge
32: end for

```

---



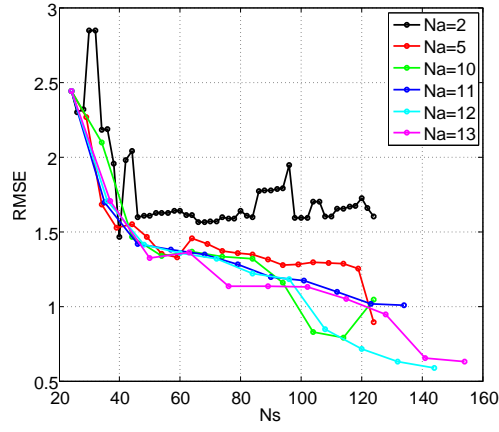
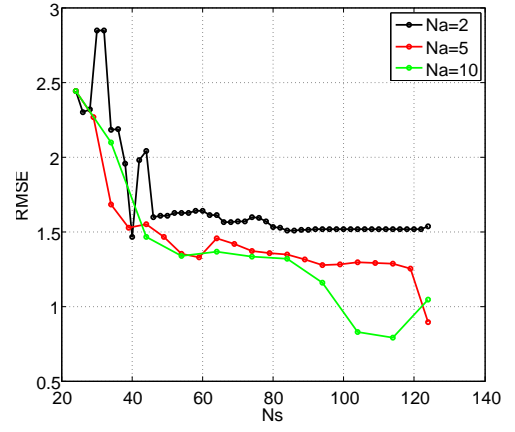
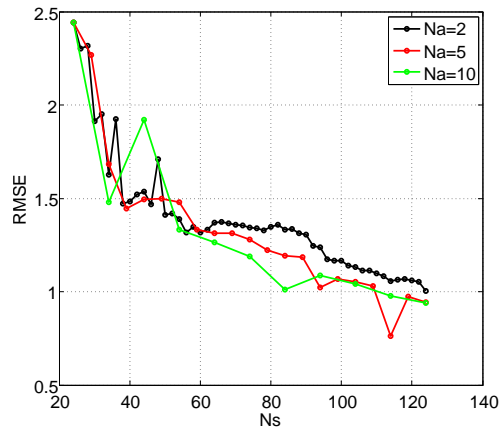
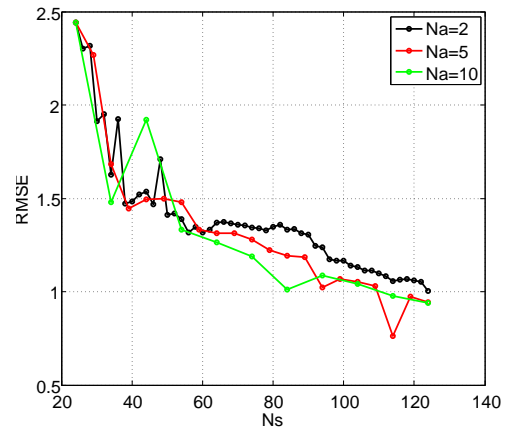
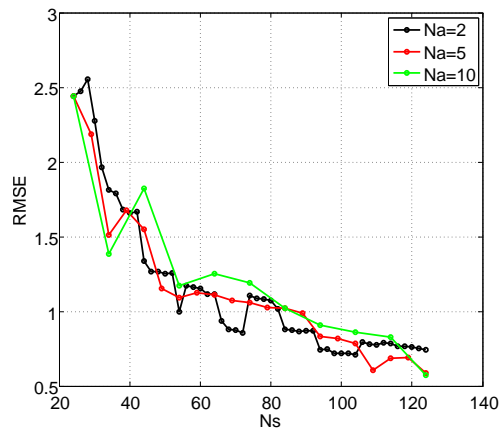
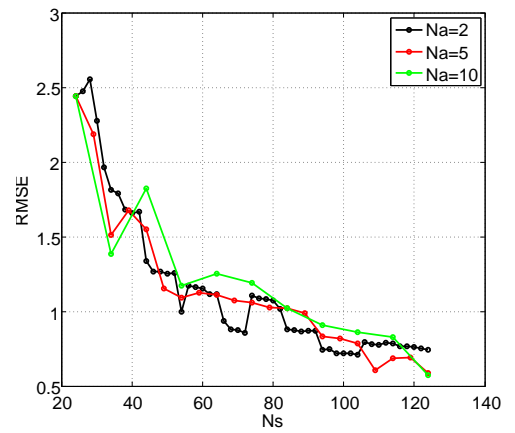
(a) brute,  $\alpha = 0.8$ (b) fast,  $\alpha = 0.8$ (c) brute,  $\alpha = 0.5$ (d) fast,  $\alpha = 0.5$ (e) brute,  $\alpha = 0.2$ (f) fast,  $\alpha = 0.2$ 

Figure 6: 2D testcase: Comparison between brute and fast approach, initial DoE of 24 points

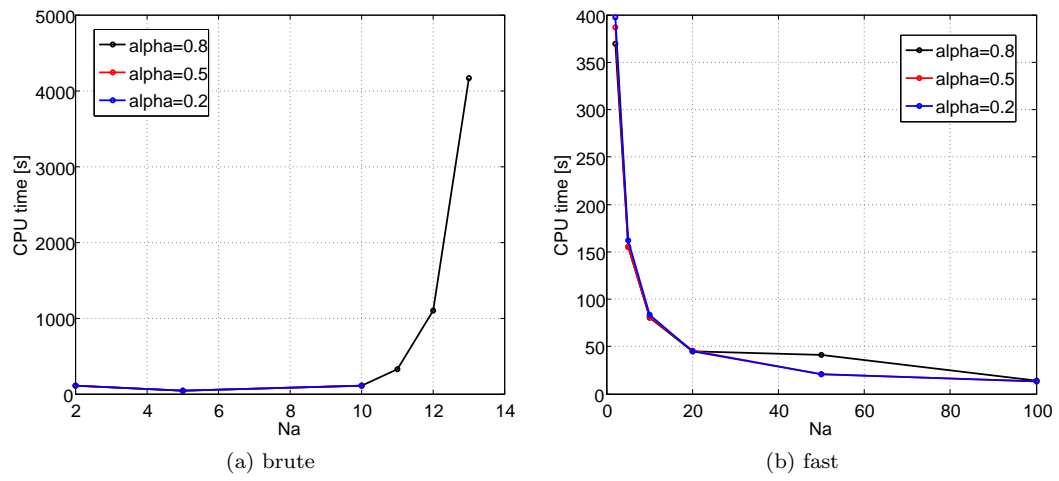


Figure 7: 2D test case: Comparison between the computational cost of brute and fast approach, initial DoE of 24 points

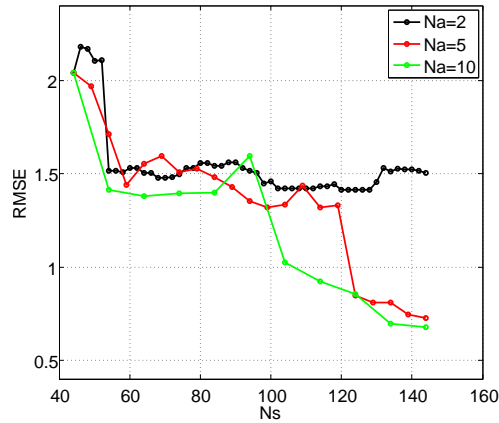
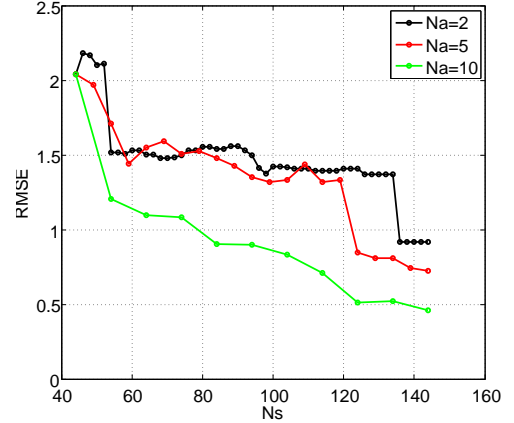
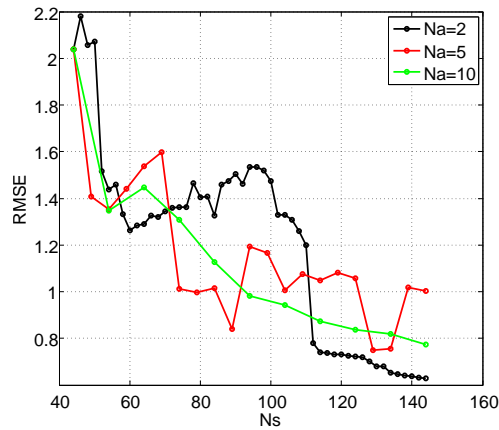
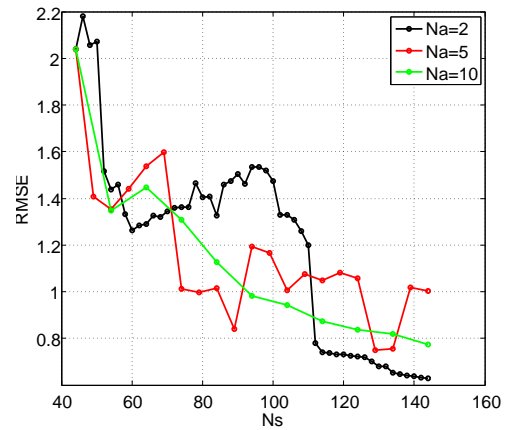
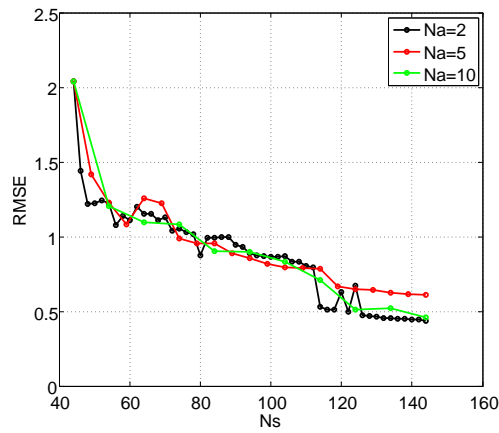
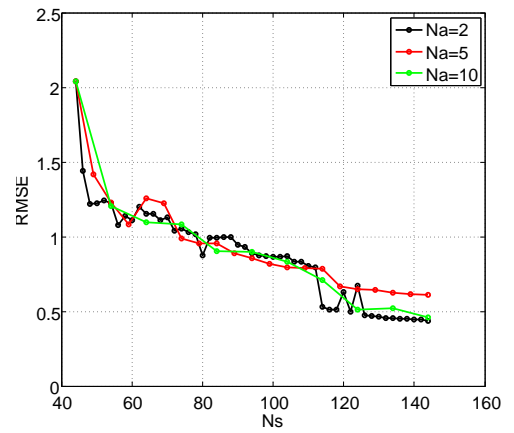
(a) brute,  $\alpha = 0.8$ (b) fast,  $\alpha = 0.8$ (c) brute,  $\alpha = 0.5$ (d) fast,  $\alpha = 0.5$ (e) brute,  $\alpha = 0.2$ (f) fast,  $\alpha = 0.2$ 

Figure 8: 2D testcase: Comparison between brute and fast approach, initial LHS of 44 points

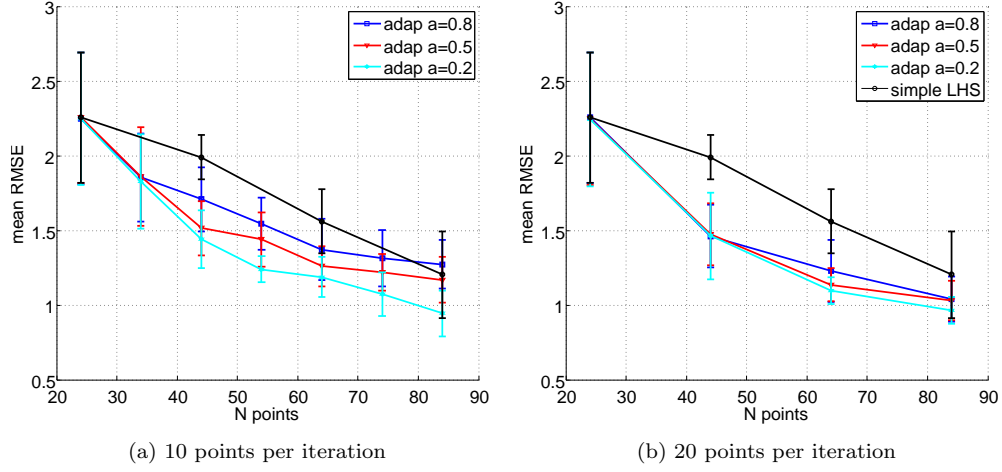


Figure 9: 2D testcase: Convergence of the mean value of the RMSE and corresponding deviation computed with 15 different starting LHS DoE. The result of a simple increase of LHS point is compared with adaptation at different values of  $\alpha$  coefficient

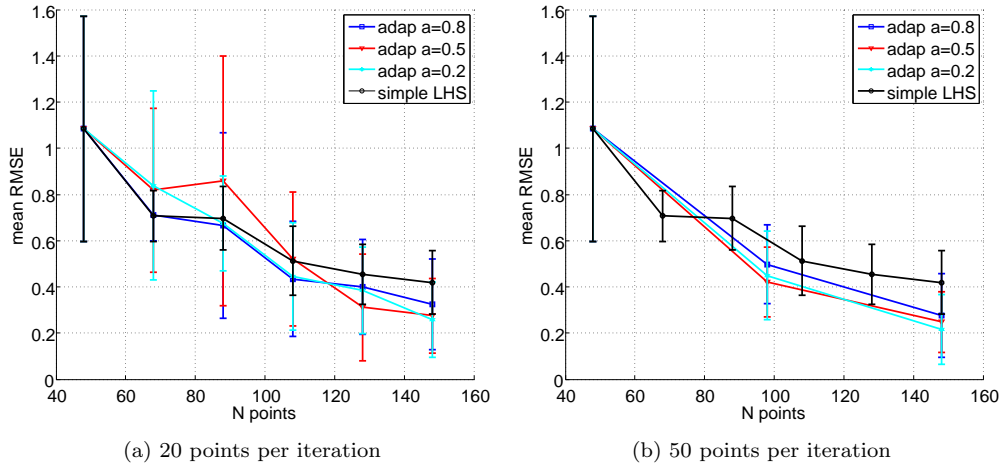


Figure 10: 3D Testcase: Convergence of the mean value of the RMSE and corresponding deviation computed with 15 different starting LHS DoE. The result of a simple increase of the LHS is compared with adaptation at different values of  $\alpha$  coefficient

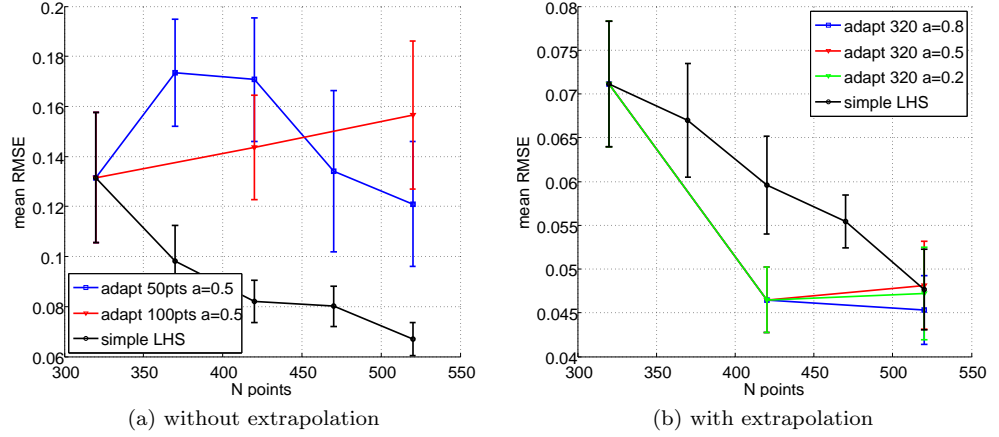


Figure 11: 8D Testcase: Convergence of the mean value of the RMSE and corresponding deviation computed with 14 different starting LHS DoE. The result of a simple increase of LHS point is compared with adaptation at different values of  $\alpha$  coefficient. A comparison is done between the normal algorithm and the one with extrapolation near the corners of the domain

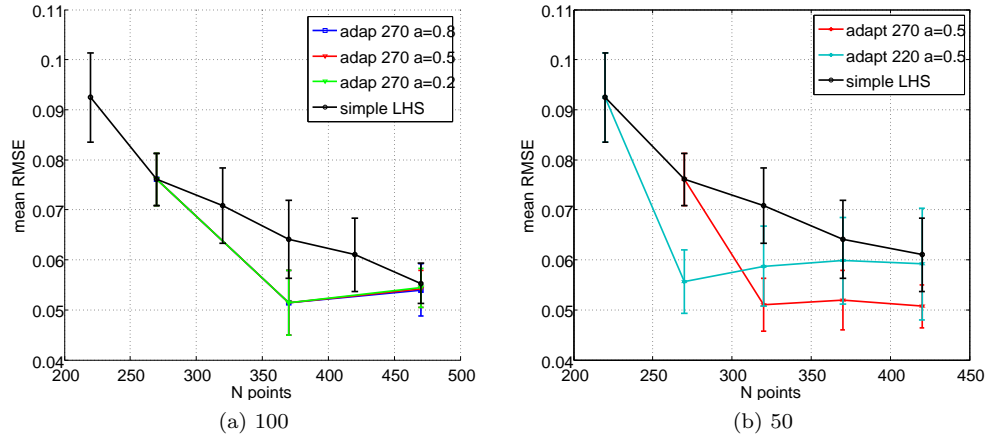


Figure 12: 8D Testcase: Convergence of the mean value of the RMSE and corresponding deviation computed with 7 different starting LHS DoE. The result of a simple increase of LHS point is compared with adaptation at different values of  $\alpha$  coefficient. A comparison is done between the addition of 100 and 50 points per iteration.

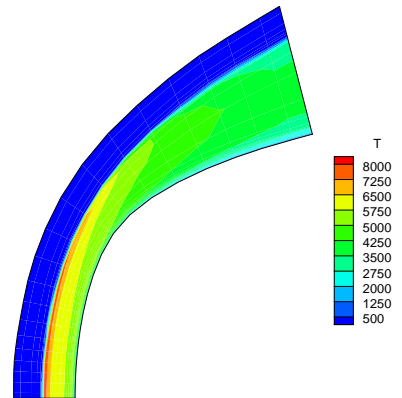


Figure 13: Simulation of the hypersonic flow around the nose of EXPERT vehicle, performed with COSMIC code: temperature field at nominal freestream conditions at 60km altitude.

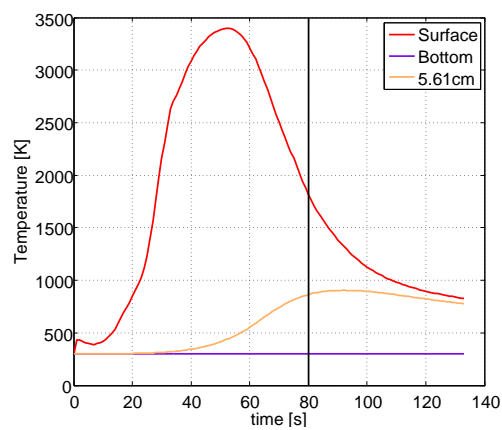


Figure 14: Temperature trend of the reference point at 5.61cm inside TACOT material compared to the one of the heated surface, obtained with nominal material parameters. The black vertical line indicates the reference time at which the sensitivity analysis is carried out.

## References

- [1] D.R Jones. A taxonomy of global optimization methods based on response surfaces. *Journal of Global Optimization*, 21:345 – 383, 2001.
- [2] O. P. Le Maître and O. M. Knio. *Spectral methods for uncertainty quantification*. Springer, 2010.
- [3] D. Xiu and G. E. Karniadakis. The wiener-asky polynomial chaos for stochastic differential equations. *SIAM J Sci Comput*, 24(2):619 – 644, 2002.
- [4] S. Rahman. A polynomial dimensional decomposition for stochastic computing. *International Journal for Numerical Methods in Engineering*, 76:2191 – 2116, 2008.
- [5] M. Buhmann. *Radial Basis Functions*. Cambridge University Press, 2003.
- [6] N. A. C. Cressie. *Statistics for spatial data*. John Wiley & Sons, 1993.
- [7] C. E. Rasmussen and C. K. I. Williams. *Gaussian processes for machine learning*. The MIT Press, 2006.
- [8] Enrica Bernardini, Seymour M.J. Spence, Daniel Wei, and Ahsan Kareem. Aerodynamic shape optimization of civil structures: A CFD-enabled Kriging-based approach. *Journal of Wind Engineering and Industrial Aerodynamics*, 144:154 – 164, 2015.
- [9] V. Dubourg and B. Sudret. Meta-model-based importance sampling for reliability sensitivity analysis. *Structural Safety*, 49:27 – 36, 2014.
- [10] B. Echard, N. Gayton, M. Lemaire, and N. Relun. A combined Importance Sampling and Kriging reliability method for small failure probabilities with time-demanding numerical models. *Reliability Engineering and System Safety*, 111:232 – 240, 2012.
- [11] Jouke de Baar, Stephen Roberts, Richard Dwight, and Benoit Mallol. Uncertainty quantification for a sailing yacht hull, using multi-fidelity kriging. *Computers and Fluids*, 123:185 – 201, 2015.
- [12] Pierre Barbillon, Gilles Celeux, Agns Grimaud, Yannick Lefebvre, and tienne De Rocquigny. Nonlinear methods for inverse statistical problems. *Computational Statistics and Data Analysis*, 55:132–142, 2011.
- [13] P. Kersaudy, B. Sudret, N. Varsier, O. Picon, and J. Wiart. A new surrogate modeling technique combining Kriging and polynomial chaos expansions - Application to uncertain analysis in computational dosimetry. *Journal of Computational Physics*, 286:103 – 117, 2015.
- [14] V. Roshan Joseph, Ying Hung, and Agus Sudjianto. Blind Kriging: A new method for developing metamodels. *ASME Journal of Mechanical Design*, (130), 2008.

- [15] K. Tang, P. M. Congedo, and R. Abgrall. Adaptive surrogate modeling by ANOVA and sparse polynomial dimensional decomposition for global sensitivity analysis in fluid simulation. *Journal of Computational Physics*, 314:557–589, 2016.
- [16] I. M. Sobol’. Sensitivity estimates for nonlinear mathematical models. *Mathematical modelling & Computational Experiments*, 1:407–414, 1993.
- [17] I. M. Sobol’. Global sensitivity indices for nonlinear mathematical models and their Monte Carlo estimates. *Mathematics and Computers in Simulations*, 55:271–280, 2001.
- [18] V. Yadav and S. Rahman. Adaptive-sparse polynomial dimensional decomposition methods for high-dimensional stochastic computing. *Comput. Methods Appl. Mech. Engrg.*, 274:56 – 83, 2014.
- [19] M. D. McKay, R. J. Beckman, and W. J. Conover. A comparison of three methods for selecting values of input variables in the analysis of output from a computer code. *Technometrics*, 21(2):239 – 245, 1979.
- [20] S. N. Lophaven, H. B. Nielsen, and J. Søndergaard. DACE: a MATLAB kriging toolbox, version 2.0. Technical report, Technical University of Denmark, 2002.
- [21] J. S. Park. Optimal latin-hypercube designs for computer experiments. *J. Stat. Plan. Inference*, 39:95 – 111, 1994.
- [22] G. G. Wang. Adaptive response surface method using inherited latin hypercube design points. *Journal of Mechanical Design*, 125:210 – 220, 2003.
- [23] J. Sacks, W. J. Welch, T. J. Mitchell, and H. P. Wynn. Design and analysis of computer experiments. *Statistical sciences*, 4(4):409 – 435, 1989.
- [24] J. A.S. Witteveen, A. Loeven, and H. Bijl. An adaptive stochastic finite elements approach based on newton-cotes quadrature in simplex elements. *Computers & Fluids*, 38:1270 – 1288, 2009.
- [25] J. A.S. Witteveen and G. Iaccarino. Refinement criteria for simplex stochastic collocation with local extremum diminishing robustness. *SIAM J. Sci. Comput.*, 34(3):A1522 – A1543, 2012.
- [26] J. A.S. Witteveen and G. Iaccarino. Simplex stochastic collocation with random sampling and extrapolation for nonhypercube probability spaces. *SIAM J. Sci. Comput.*, 34(2):A814 – A838, 2012.
- [27] J. A.S. Witteveen and G. Iaccarino. Simplex stochastic collocation with ENO-type stencil selection for robust uncertainty quantification. *Journal of Computational Physics*, 239:1 – 21, 2013.
- [28] Charles Audet and Jr. J. E. Dennis. Mesh adaptive direct search algorithms for constrained optimization. *SIAM Journal on Optimization*, 17(1):188–217, 2006.
- [29] H.-M. Gutmann. A radial basis function method for global optimization. *Journal of Global Optimization*, 19(3):201–227, 2001.



- [30] Rommel G. Regis and Christine A. Shoemaker. A stochastic radial basis function method for the global optimization of expensive functions. *INFORMS Journal on Computing*, 19(4):497–509, 2007.
- [31] Rommel G. Regis. Stochastic radial basis function algorithms for large-scale optimization involving expensive black-box objective and constraint functions. *Comput. Oper. Res.*, 38(5):837–853, May 2011.
- [32] Stefan Jakobsson, Michael Patriksson, Johan Rudholm, and Adam Wojciechowski. A method for simulation based optimization using radial basis functions. *Optimization and Engineering*, 11(4):501–532, 2010.
- [33] T. Coupez. Metric construction by length distribution tensor and edge based error for anisotropic adaptive meshing. *Journal of Computational Physics*, 230:2391 – 2405, 2011.
- [34] T. Coupez, G. Jannoun, N. Nassif, H.C. Nguyen, H. Digonnet, and E. Hachem. Adaptive time-step with anisotropic meshing for incompressible flows. *Journal of Computational Physics*, 241:195 – 211, 2013.
- [35] A. Conn, K. Scheinberg, and L. Vicente. *Introduction to Derivative-Free Optimization*. Society for Industrial and Applied Mathematics, 2009.
- [36] G. Matheron. *The theory of regionalised variables and its applications*. PhD thesis, cole Nationale Suprieure des Mines, 1971.
- [37] V. Picheny. *Improving accuracy and compensating for uncertainty in surrogate modeling*. PhD thesis, cole Nationale Suprieure des Mines, 2009.
- [38] P. G. Constantine, E. Dow, and Q. Wang. Active subspace method in theory and practice: application to kriging surfaces. *SIAM J. Sci. Comput.*, 36(4):A1500 – A1524, 2014.
- [39] Luca Margheri and Pierre Sagaut. A hybrid anchored-ANOVA POD/kriging method for uncertainty quantification in unsteady high-fidelity CFD simulations. *Journal of Computational Physics*, 324:137 – 173, 2016.
- [40] Abdellah Chkifa, Albert Cohen, Pierre-Yves Passaggia, and Jacques Peter. A comparative study between kriging and adaptive sparse tensor-product methods for multi-dimensional approximation problems in aerodynamics design. *ESAIM: PROCEEDINGS AND SURVEYS*, 48:248–261, 2015.
- [41] D.R Jones, M. Schonlau, and W. J. Welch. Efficient global optimization of expensive black-box functions. *Journal of Global Optimization*, 13:455 – 492, 1998.
- [42] J. Tryoen, P. M. Congedo, R. Abgrall, N. Villedieu, and T.E. Magin. Bayesian-based method with metamodels for rebuilding freestream conditions in atmospheric entry flows. *AIAA Journal*, 52(10):2190 – 2197, 2014.
- [43] P. Barbante. *Accurate and efficient modelling of high temperature non-equilibrium air flows*. PhD thesis, Von Karman Institute, 2001.

- [44] C. Park, R. Jaffe, and H. Partridge. Chemical-kinetic parameters of hyperbolic earth entry. *Journal of Thermophysics and Heat Transfer*, 15(1):76 – 90, 2001.
- [45] B. Van Leer. Towards the ultimate conservative difference scheme. V. A second-order sequel to godunov’s method. *Journal of Computational Physics*, 32(1):101–136, 1979.
- [46] S. Osher and F. Solomon. Upwind Difference Schemes for Hyperbolic Systems of Conservation Laws. *Mathematics of Computation*, 38(158):339–374, 1982.
- [47] B. Bottin, O. Chazot, M. Carbonaro, V. Van Der Haegen, and S. Paris. *The VKI Plasmatron Characteristics and Performance*. Defense Technical Information Center, 2000.
- [48] Jean Lachaud and Nagi N. Mansour. Porous-material analysis toolbox based on openfoam and applications. *Journal of Thermophysics and Heat Transfer*, 28(2):191–202, 2014.
- [49] T. Goel, R. T. Haftka, and W. Shyy. Comparing error estimation measures for polynomial and kriging approximation of noise-free functions. *Structural and multidisciplinary optimization*, 38:429 – 442, 2009.
- [50] M. Meckesheimer, R. R. Barton, T. W. Simpson, and A. Booker. Computationally inexpensive metamodel assessment strategies. *AIAA Journal*, 40(10):2053 – 2060, 2002.



**RESEARCH CENTRE  
BORDEAUX – SUD-OUEST**

351, Cours de la Libération  
Bâtiment A 29  
33405 Talence Cedex

Publisher  
Inria  
Domaine de Voluceau - Rocquencourt  
BP 105 - 78153 Le Chesnay Cedex  
[inria.fr](http://inria.fr)

ISSN 0249-6399